Dalton Transactions

Accepted Manuscript

ROYAL SOCIETY OF CHEMISTRY

www.rsc.org/dalton

Journal Name

RSCPublishing

ARTICLE

Magneto-Structural Variety of New 3d-4f-4(5)d Heterotrimetallic Complexes

Cite this: DOI: 10.1039/x0xx00000x

Diana Visinescu[a,*], Maria-Gabriela Alexandru[b], Augustin M. Madalan[b], Céline Pichon[c,d], Carine Duhayon[c,d], Jean-Pascal Sutter[c,d*] and Marius Andruh[b,*]

Received 00th January 2012,
Accepted 00th January 2012

DOI: 10.1039/x0xx00000x

www.rsc.org/

Three families of heterotrimetallic chains (**Type 1** - **Type 3**), with different topologies, have been obtained by reacting the 3d-4f complexes, $[\{Cu(L^1)\}_xLn(NO_3)_3]$ with x = 1 or 2, formed *in situ* by reaction of Schiff-base bi-compartmental $[Cu^{II}(L^1)]$ complexes and lanthanide(III) salts, with $(NHBu_3)_3[M(CN)_8]$ (M = Mo^V, W^V). For **type 1** series of compounds, 1-D coordination polymers, with the general formula $[\{Cu_2(valpn)_2Ln\}\{M(CN)_8\}]\cdot nH_2O\cdot mCH_3CN$ (where H_2valpn = 1,3-propanediylbis(2-iminomethylene-6-methoxy-phenol), result from the association of trinuclear $\{Cu_2^{II}Ln^{III}\}$ trinuclear moieties and $[M^V(CN)_8]^{3-}$ anions acting as a tri-connecting spacers [Ln = La (**1**), Ce (**2**), Eu (**3**), Tb (**4**), Ho (**5**), M = Mo; Ln = Tb (**6**), Ho (**7**), M = W; m = 0, n =1 (**5**), 1.5 (**7**) and n = 2 (**1-4**, **6**); m = 1 (**5**)]. **Type 2** family has the general formula $[\{Cu(valdp)Ln(H_2O)_4\}\{M(CN)_8\}]\cdot 2H_2O\cdot CH_3CN$ (where H_2valdp = 1,2-propanediylbis(2-iminomethylene-6-methoxy-phenol) and also consists in heterotrimetallic chains but involving binuclear $\{Cu^{II}Ln^{III}\}$ units linked to $[M(CN)_8]^{3-}$ anions coordinating through two cyano groups [Ln = Gd (**8**), Tb (**9**), Dy (**10**); M = Mo; Ln = La (**11**), Gd (**12**), Tb (**13**), Dy (**14**); M = W]. With large Ln^{III} ions (La^{III} and Pr^{III}), the **type 3** family of heterotrimetallic compounds are assembled: $[\{Cu_2(valdp)_2Ln(H_2O)_4\}\{Mo(CN)_8\}]\cdot nCH_3OH\cdot mCH_3CN$, n, m = 0, Ln = La (**15**); n = m = 1, Pr (**16**), in which the trinuclear $\{Cu_2^{II}Ln^{III}\}$ nodes are connected to $[Mo^V(CN)_8]^{3-}$ anions, that act as tetra-connecting spacers. For Tb^{III} derivatives of **type 1** family (compounds **4** and **6**), the DC magnetic properties indicate a predominant ferromagnetic Cu^{II}-Tb^{III} interaction, while the AC magnetic susceptibility (in the presence of a static magnetic field, H_{DC} = 3000 Oe) emphasize the slow relaxation of the magnetization (U_{eff}/k_BT = 20.55 K and $\tau_0 = 5.5\cdot10^{-7}$ s for compound **4**, U_{eff}/k_BT = 15.1 K and τ_0 = 1.5 10^{-7} s for compound **6**). A predominant ferromagnetic Cu^{II}-Ln^{III} interaction was also observed in the **type 2** series (compounds **8-10** and **12-14**) as a result of the magnetic coupling between copper(II) and lanthanide(III) ions *via* the phenoxo-bridge. The magnetic behavior for the La^{III} derivatives reveals that weak ferromagnetic interactions are also operative between the Cu^{II} and the 4d/5d centers.

Introduction

The interest in the chemistry of polynuclear complexes arises from their rich properties that make them very attractive for obtaining molecule-based materials: porous systems,[1] catalysts,[2] luminophores for photo- and electroluminescent devices,[3] or magnetic materials.[4] The rational design of heterometallic complexes marked a step forward in the developement of molecular magnetism. The presence of two or more paramagnetic metal ions within the same molecular entity, with a specific spin topology, leads to diverse and interesting magnetic phenomena, such as ferro- and ferrimagnetism,[5] complexes showing irregular spin-state structures[6] or molecular magnets with high T_c.[7] More recently, numerous heterometallic complexes with high-spin ground states and magnetic anisotropy were found to show slow relaxation of the magnetization (Single-Molecule Magnet, SMMs and Single-Chain Magnets, SCMs).[8] In this respect, an important goal in molecular magnetism is to design, synthesize and explore the properties of new classes of heterometallic nanomagnets relevant for applications such as high-density storage devices or molecular electronics.[9]

The useful concepts of metallo-supramolecular chemistry have stimulated the development of bottom-up methods, which

are efficient in controlling the nuclearity or dimensionality of the desired polynuclear complexes. Heterobimetallic complexes were largely exploited to generate molecule-based magnets.[10] The forthcoming step, namely complexes with three different spin carriers, represents an alternative way to design high-spin molecules. The access to such compounds is not straightforward and heterotrimetallic complexes are rather rare species. Since the first examples reported by Chaudhuri *et al.,*[11] only *ca*. 60 examples of heterotrimetallic complexes were reported to date. Several interesting heterotrimetallic compounds have been obtained serendipitously, from one-pot reactions.[12] However, such procedures are difficult to be expanded into synthetic strategies especially because of the formation of mixtures of different compounds. The scrambling of the metal ions represents another difficulty in the synthesis of such compounds, and can be avoided using stepwise approaches. Ones of the first examples of designed heterotrimetallic complexes were the two-dimensional coordination polymers obtained from the reaction of pre-formed rigid oxamidato-based complexes with anionic complexes with potentially bridging ligands (metallo-ligands).[13] Linear trinuclear $\{M_2^{II}Ln^{III}L\}$ complexes (M = Co, Cu; Ln = La, Gd, L = 2,6-di(acetoacetyl)pyridine) also provided suitable platforms to assemble heterotrimetallic 3-D molecular magnets or SCMs.[14]

A very efficient strategy for the synthesis of systems carrying three different paramagnetic metal ions, largely developed by us, consists in the self-assembly process involving heterobimetallic complexes with Schiff-base compartmental ligands[15] (macrocyclic[16, 17] or side-off type[18-23]) and oxalato- or cyano-based metallo-ligands. The success of this strategy is mainly due to the availability of a rich library of 3d-3d' or 3d-4f heterobimetallic complexes with compartmental ligands that can be used as precursors.[24] The complexes involving transition and rare-earth ions are particularly interesting for the design of heterotrimetallic nanomagnets because: (i) the exchange interaction between the 3d and 4f ions is often ferromagnetic;[25] (ii) trivalent 4f cations bring large magnetic moments and, (iii) in the case of Ln^{III} = Dy, Tb, Ho strong magnetic anisotropy.[26] As a result, many heterobimetallic complexes containing phenoxo-bridged Cu^{II}-Ln^{III} or Ni^{II}-Ln^{III} pairs (Ln^{III} = Tb, Dy) exhibit SMM properties.[27]

Cyano-based complexes of the second and third transition metal rows became very popular building-blocks in designing molecular magnetic materials.[28] Paramagnetic Mo^V/W^V polycyano anions, proved to be efficient units to form cyano-bridged heteropolymetallic assemblies with substantial exchange interactions due to the more diffuse 4(5)d magnetic orbitals.[29] The variable geometry and versatile coordination modes of these metallo-ligands led to discrete polynuclear complexes or extended structures with various network topologies.[30] The Mo^V/W^V-containing cyanometallate anions are increasingly employed in the aggregation of 3d-4f-4(5)d type heterotrimetallic systems, generating either oligonuclear complexes or chains.[14b, 19-21]

The slight structural modifications of the Schiff-base ligand correlated with different possible coordination modes of the octacyanometallate units influence the topology and dimensionality of the resulting heterotrimetallic complexes.[20] For example, by using $valpn^{2-}$ as ligand (H_2valpn = 1,3-propanediylbis(2-iminomethylene-6-methoxy-phenol), we obtained 3d-4f-4(5)d heterotrimetallic chains, in which the $\{Cu^{II}_2Ln^{III}\}$ trinuclear moieties are linked by $\{M^V(CN)_8\}$ spacers (M = Mo, W).[20a] A more rigid compartmental ligand, $valen^{2-}$ (H_2valen = *N,N'*-ethylenediaminato bis(3-methoxyiminate) ligand), gave rise either to a zigzag 1-D coordination polymer or a discrete trinuclear complex, made up from binuclear $\{Cu^{II}Ln^{III}\}$ units and $[W(CN)_8]^{3-}$ metallo-ligands.[20b]

Subtle factors such as the nature of the ligands, the size (ionic radii) of 4f ions may account for the various structural topology and dimensionality of these heterotrimetallic systems. In order to reveal their effective influence, we have examined a series of $\{Cu^{II}Ln^{III}\}$ Schiff-base complexes with various Ln^{III} ions and two types of Schiff-bases ligands, namely $valpn^{2-}$ and $valdp^{2-}$ (H_2valdp = 1,2-propanediylbis(2-iminomethylene-6-methoxy-phenol). The resulting 3d-4f-4(5)d heterotrimetallic chains have been systematically characterized and their magnetic behaviors investigated.

Experimental

Materials. The chemicals used, i.e. *o*-vanillin, 1,3-diaminopropane and 1,2-diaminopropane, and $Ln(NO_3)_3 \cdot xH_2O$, as well as the acetonitrile were of reagent grade and were purchased from commercial sources. [Cu(valpn)], [Cu(valdp)][18b] and $(NHBu_3)[M(CN)_8]\cdot 2H_2O$[31] (M = Mo, W) were prepared as described in literature.

Synthesis of the heterotrimetallic compounds.

Type 1. Complexes **1**-**7** were obtained following the same general method: an acetonitrile solution (20 cm^3) of $(NHBu_3)_3[M(CN)_8]\cdot 2H_2O$ (0.04 mmol, M = Mo, W) was poured into another acetonitrile solution (20 cm^3) containing [Cu(valpn)] (0.037 mmol) or [Cu(valdp)] and the corresponding lanthanide salt, $Ln(NO_3)_3 \cdot 6H_2O$ (0.034 mmol) [Ln = La (**1**), Ce (**2**), Eu(**3**), Tb (**4**), Ho (**5**), M = Mo; Ln = Tb (**6**), Ho (**7**), M^V = W]. Slow evaporation of the green solutions at room temperature afforded, after a few days, green prisms for all compounds belonging to **type 1** family (compounds **1**-**7**). Anal. Calcd for $C_{46}H_{44}Cu_2LaMoN_{12}O_{10}$ (**1**): C, 42.89; H, 3.41; N, 13.05. Found: C, 42.70; H, 3.01; N, 13.20 % (Yield = 60 %). Anal. Calcd/ for $C_{46}H_{44}Cu_2CeMoN_{12}O_{10}$ (**2**): C, 42.85; H, 3.41; N, 13.04. Found: C, 42.31; H, 3.15; N, 13.50 % (Yield = 55 %). Anal. Calcd. for $C_{46}H_{44}Cu_2EuMoN_{12}O_{10}$ (**3**): C, 42.46; H, 3.38; N, 12.92. Found: C, 42.75; H, 3.10; N, 13.31 % (Yield 44 %). Anal. Calcd. for $C_{46}H_{44}Cu_2TbMoN_{12}O_{10}$ (**4**): C, 42.23; H, 3.36; N, 12.85. Found: C, 42.5; H, 3.30; N, 13.51 % (Yield 70 %). Anal. Calcd. for $C_{48}H_{45}Cu_2HoMoN_{13}O_9$ (**5**): C, 43.11; H, 3.36; N, 13.62. Found: C, 42.95; H, 3.34; N, 13.5 % (Yield = 60 %).

Journal Name RSCPublishing

ARTICLE

Table 1. Crystal data and details of the crystal determinations for compounds **1-6** (**Type 1**).

	1	**2**	**3**	**4**	**5**	**6**
Empirical formula	$C_{46}H_{44}Cu_2LaMoN_{12}O_{10}$	$C_{46}H_{44}Cu_2CeMoN_{12}O_{10}$	$C_{46}H_{44}Cu_2EuMoN_{12}O_{10}$	$C_{46}H_{44}Cu_2TbMoN_{12}O_{10}$	$C_{47.30}H_{44.65}Cu_2HoMoN_{12.65}O_{9.35}$	$C_{46}H_{44}Cu_2TbWN_{12}O_{10}$
M (g mol^{-1})	1286.86	1288.07	1299.91	1306.87	1327.85	1394.78
Temperature (K)	293(2)	293(2)	293(2)	293(2)	293(2)	293(2)
Wavelength (Å)	0.71073	0.71073	0.71073	0.71073	0.71073	0.71073
Crystal system	Triclinic	Triclinic	Triclinic	Triclinic	Triclinic	Triclinic
Space group	*P-1*	*P-1*	*P-1*	*P-1*	*P-1*	*P-1*
a(Å)	11.4503(6)	11.476(1)	11.4089(4)	11.4193(7)	11.362(1)	11.3977(5)
b(Å)	12.4739(7)	12.451(1)	12.4074(5)	12.3706(9)	12.446(1)	12.3689(6)
c (Å)	20.7387(12)	20.805(2)	20.6391(9)	20.607(2)	21.282(2)	20.536(1)
α (^{o})	94.775(4)	94.748(7)	94.967(3)	95.112(6)	105.814(7)	95.088(4)
β (^{o})	102.112(4)	102.203(7)	102.028(3)	101.921(5)	92.659(7)	101.795(4)
γ (^{o})	115.971(4)	116.332(6)	116.494(3)	116.803(5)	116.095(7)	116.645(3)
V (Å^3)	2551.5(3)	2550.7(4)	2502.9(2)	2486.2(3)	2551.8(4)	2478.6(2)
Z	2	2	2	2	2	2
D_c (g cm^{-3})	1.675	1.677	1.725	1.746	1.728	1.869
μ (mm^{-1})	1.950	2.005	2.387	2.564	2.664	4.638
F(000)	1282	1284	1294	1298	1318	1362
Refinement on	F^2	F^2	F^2	F^2	F^2	F^2
Goodness of fit	1.078	0.877	1.068	0.926	0.894	0.955
Final R indices	R_1 = 0.0545	R_1 = 0.0514	R_1 = 0.0549	R_1 =0.0548	R_1 = 0.0487	R_1 = 0.0530
[I>2σ(I)]	wR_2 = 0.1164	wR_2 = 0.0694	wR_2 = 0.1301	wR_2 = 0.1012	wR_2= 0.0989	wR_2 = 0.1051
R indices (all data)	R_1= 0.0812	R_1 = 0.0805	R_1 = 0.0728	R_1 = 0.1067	R_1 = 0.0872	R_1 = 0.1003
	wR_2= 0.1254	wR_2= 0.1117	wR_2= 0.1383	wR_2= 0.1174	wR_2=0.1086	wR_2= 0.1194

Anal. Calcd. for $C_{46}H_{44}Cu_2TbWN_{12}O_{10}$ (**6**): C, 39.57; H, 3.15; N, 12.04. Found: C, 40.51; H, 3.10; N, 12.45 % (Yield = 35 %). Anal. Calcd. for $C_{46}H_{40}Cu_2HoWN_{12}O_{9.5}$ (**7**): C, 39.66; H, 2.87; N, 12.07. Found: C, 40.72; H, 3.12; N, 12.52 % (Yield = 55 %). Main IR peaks (cm^{-1}): 3422 (m) (**1**), 3435 (m) (**2**), 3446 (m) (**3**), 3430 (m) (**4**), 3468 (m) (**5**), 3440 (m) (**6**), 3448 (m) (**7**), $\nu(C\equiv N)_{cyano}$: 2157 (m), 2143 (m), 2090 (m) (**1**); 2158 (m), 2145 (m), 2108 (m) (**2**); 2163 (m), 2143 (m), 2107 (m) (**3**); 2167 (m), 2143 (m), 2111 (m) (**4**); 2165 (m), 2143 (m), 2110 (m) (**5**); 2168 (m), 2144 (m), 2100 (m) (**6**); 2168 (m), 2144 (m), 2106 (m) (**7**); $\nu(C=N)_{imine}$: 1627 (s), 1474 (s) (**1**); 1627 (s), 1474 (s) (**2**); 1628 (s), 1474 (s) (**3**); 1628 (s), 1474 (s) (**4**); 1627 (s), 1475 (s) (**5**); 1627 (s), 1472 (s) (**6**); 1627 (s), 1474 (s) (**7**).

Type 2. Red-brownish prisms of compounds **9-14** have been obtained following a similar procedure as for **type 1** series [Ln = Gd (**8**), Tb (**9**), Dy (**10**); M = Mo; Ln = La (**11**), Gd (**12**), Tb (**13**), Dy (**14**); M = W]. Anal. Calcd. for $C_{29}H_{35}CuGdMoN_{11}O_{10}$ (**8**): C, 34.30; H, 3.45; N, 15.18 Found: C, 33.5; H, 3.5; N, 14.89 % (Yield = 80 %). Anal. Calcd. for $C_{29}H_{35}CuTbMoN_{11}O_{10}$ (**9**): C, 34.24; H, 3.44; N, 15.15. Found: C, 34.5; H, 3.14; N, 15.65 % (Yield = 35 %). Anal. Calcd. for $C_{29}H_{35}CuDyMoN_{11}O_{10}$ (**10**): C, 34.12; H, 3.43; N, 15.10. Found: C, 34.5; H, 3.6; N, 15.83 % (Yield = 45 %). Anal. Calcd. for $C_{29}H_{35}CuLaWN_{11}O_{10}$ (**11**): C, 32.10; H, 3.22; N, 14.20. Found: C, 33.46; H, 3.42; N, 15.05 % (Yield = 35 %). Anal. Calcd. for $C_{29}H_{35}CuGdWN_{11}O_{10}$ (**12**): C, 31.56; H, 3.17; N, 13.97. Found: C, 32.48; H, 3.15; N, 14.34 % (Yield = 70 %). Anal. Calcd. for $C_{29}H_{35}CuTbWN_{11}O_{10}$ (**13**): C, 31.52; H, 3.17; N, 13.94. Found: C, 32.12; H, 3.18; N, 14.23 % (Yield = 45 %). Anal. Calcd. for $C_{29}H_{35}CuDyWN_{11}O_{10}$ (**14**): C, 31.42; H, 3.16; N, 13.90. Found: C, 31.97; H, 3.35; N, 13.87 % (Yield = 70 %). Main IR peaks (cm^{-1}): 3450 (m) (**8**), 3489 (m) (**9**), 3456 (m) (**10**), 3485 (m) (**11**), 3487 (m) (**12**), 3470 (m) (**13**), 3485 (m) (**14**); $\nu(C\equiv N)_{cyano}$: 2176 (m), 2161(w), 2133 (m), 2112 (m) (**8**); 2178 (m), 2163(w), 2137 (m), 2116 (m) (**9**); 2179 (m), 2137 (m), 2115 (w) (**10**); 2176 (m), 2140 (m), 2110 (w) (**11**); 2180 (m), 2138 (m), 2106 (w) (**12**); 2181 (m), 2137 (m), 2105 (w) (**13**); 2181 (m), 2138 (m), 2105 (w) (**14**); $\nu(C=N)_{imine}$: 1654 (m), 1637 (s), 1605(m), 1476 (s) (**8**); 1655 (m), 1638 (s), 1606(m), 1475 (s) (**9**); 1637 (s), 1609 (m), 1480 (m) (**10**); 1635 (s), 1605 (m), 1472 (m) (**11**); 1635 (s), 1607 (m), 1473 (m) (**12**); 1637 (s), 1607 (m), 1474 (m), (**13**); 1636 (s), 1607 (m), 1472 (m) (**14**). Cell parameters for **7** determined at 180 K: a = 11.3579(12), b = 12.3025(12), c = 20.370(2) Å, α = 94.844(12), β = 101.897(12), γ = 116.662(11)^o, V = 2437.6(4) Å^3. Cell parameters for **8** and **9** determined at 173(2) K: a = 9.13 (**8**) and 9.16 (**9**) Å, b = 20.29 (**8**) and 20.35 (**9**) Å, c = 10.41 (**8**) and 10.40 (**9**) Å, β = 96.95 (**8**) and 96.60 (**9**)^o, V = 1916 (**8**) and 1928 (**9**) Å^3.

Table 2. Crystal data and details of the crystal determinations for compounds **10-14** (**Type 2**) and **15 (Type 3)**

	10	**11**	**12**	**13**	**14**	**15**
Empirical formula	$C_{29}H_{35}CuDyMoN_{11}O_{10}$	$C_{29}H_{35}CuLaWN_{11}O_{10}$	$C_{29}H_{35}CuGdWN_{11}O_{10}$	$C_{29}H_{35}CuTbWN_{11}O_{10}$	$C_{29}H_{35}CuDyWN_{11}O_{10}$	$C_{46}H_{40}Cu_2LaMoN_{12}O_8$
M (g mol^{-1})	1019.66	1083.98	1102.32	1103.99	1107.57	1250.83
Temperature (K)	173(2)	173(2)	293(2)	293(2)	293(2)	293(2)
Wavelength (Å)	0.71073	0.71073	0.71073	0.71073	0.71073	0.71073
Crystal system	Monoclinic	Monoclinic	Monoclinic	Monoclinic	Monoclinic	Orthorhombic
Space group	$P2_1$	$P2_1$	$P2_1$	$P2_1$	$P2_1$	$C222_1$
a(Å)	9.0527(5)	9.2526(5)	9.1369(3)	9.1488(18)	9.1370(9)	15.6813(10)
b(Å)	20.2580(8)	20.3849(11)	20.3271(9)	20.356(4)	20.3334(14)	19.0221(17)
c (Å)	10.3391(5)	10.4325(5)	10.3756(3)	10.386(2)	10.3859(10)	17.6117(10)
β (^{o})	96.115(4)	96.692(4)	96.597(3)	96.69(3)	96.566(8)	90
V (Å^3)	1885.29(16)	1954.30(18)	1914.27(12)	1921.0(7)	1916.9(3)	5253.4(6)
Z	2	2	2	2	2	4
D_c (g cm^{-3})	1.796	1.842	1.912	1.909	1.919	1.581
μ (mm^{-1})	2.915	4.613	5.326	2.564	5.538	1.889
F(000)	1006	1052	1066	1068	1070	2484
Refinement on	F^2	F^2	F^2	F^2	F^2	F^2
Goodness of fit	0.977	0.990	1.000	0.889	0.695	0.910
Final R indices	R_1 = 0.0316	R_1 = 0.0678	R_1 = 0.0318	R_1 = 0.0444	R_1 = 0.0491	R_1 = 0.0471
[I>2σ(I)	wR_2 = 0.0652	wR_2 = 0.1569	wR_2 = 0.0712	wR_2 = 0.0754	wR_2 = 0.0703	wR_2 = 0.0790
R indices (all data)	R_1 = 0.0378 wR_2 = 0.0666	R_1 = 0.0945 wR_2 = 0.1694	R_1 = 0.0375 wR_2 = 0.0727	R_1 = 0.0670 wR_2 = 0.0806	R_1 = 0.1239 wR_2 = 0.0909	R_1 = 0.0758 wR_2 = 0.0863

Type 3. Dark-red prisms of **type 3** series (compounds **15** and **16**) have been synthesized in a similar way, except for **16** in which the reaction was carried out in methanol:acetonitrile solution (v/v = 1:10) [Ln = La (**15**), Pr (**16**), M = Mo]. Anal. Calcd. for $C_{46}H_{40}Cu_2LaMoN_{12}O_8$ (**15**): C, 44.13; H, 3.19; N, 13.43. Found: C, 42.94; H, 3.42;N, 13.54% (Yield = 30 %). Anal. Calcd. for $C_{49}H_{47}Cu_2PrMoN_{13}O_9$ (**16**): C, 44.34; H, 3.54; N, 13.72. Found: C, 44.52; H, 3.67; N, 13.78 % (Yield = 20 %). Main IR peaks (cm^{-1}): 3482 (m) (**15**), 3445 (m) (**16**); $\nu(C\equiv N)_{cyano}$: 2159 (m), 2142 (m), 2110 (w) (**15**); 2180 (m), 2142 (m), 2110 (w) (**16**); $\nu(C=N)_{imine}$: 1636 (s), 1606 (m), 1455 (m) (**15**); 1640 (s), 1610 (m), 1462 (m) (**16**).

Physical Measurements. The IR spectra of **1-16** were recorded on a FTIR Bruker Tensor V-37 spectrophotometer as KBr pellets in the 4000-400 cm^{-1} range. Magnetic measurements were carried out with a Quantum design MPMS-5S SQUID magnetometer in the temperature range from 2 to 300 K. The measurements were performed on crushed crystals from freshly isolated samples to avoid solvent loss. The powders were mixed with grease and put in gelatin capsules. The magnetic susceptibilities were measured in an applied field of 1000 Oe. The molar susceptibility (χ_M) was corrected for the sample holder and for the diamagnetic contribution of all the atoms using Pascal's tables. The ac susceptibility was measured with an oscillating ac field of 3 Oe in the frequency range from 1 to 1500 Hz.

Crystallographic Data Collection and Structure Determination. Suitable single crystals of compounds **1-6** and **8-16** were mounted on an IPDS II STOE diffractometer, and, for compound **7**, on an IPDS STOE diffractometer. Diffraction data for the compounds were collected at 293(2) or 173(2) K using graphite-monochromated Mo-Kα radiation (λ = 0.71073 Å). Multi-scan absorption corrections were applied except for **7** for which no improvement of the refinement was found. The structures were solved by direct methods using SHELXS-2014, SHELXS-97, SIR92, or SUPERFLIP and refined by means of least-squares procedures using the programs of the PC version of SHELXL-2014, SHELXL-97 or CRYSTALS. Atomic scattering factors were taken from the international tables for X-ray crystallography. Hydrogen atoms were included but not refined. In the crystal structures of the compounds **10-13** there is a degree of disorder (less than 15-20%) on the backbone C9A-C9-C10 derived from 1,2-diaminopropane but we couldn't find a good model for this disorder. Crystal **15** contains solvent accessible voids and the solvent accessible volume found by SQUEEZE was 872.4 A^3 with an electron count of 117 in this volume. The structure was refined using the hkl file generated by SQUEEZE. Drawings of the molecule were performed with the program Diamond 3. A summary of the crystallographic data and the structure refinement parameters is given in Tables 1-2 and Table S1 (compound **16**) in ESI. CCDC reference numbers are as follows: 1060172 (**1**), 1060173 (**2**), 1060174 (**3**), 1060175 (**4**), 1060176 (**5**),1060177 (**6**), 1060179 (**10**), 1060180 (**11**), 1060181 (**12**), 1060182 (**13**), 1060183 (**14**), 1060184 (**15**) and 1060185 (**16**).

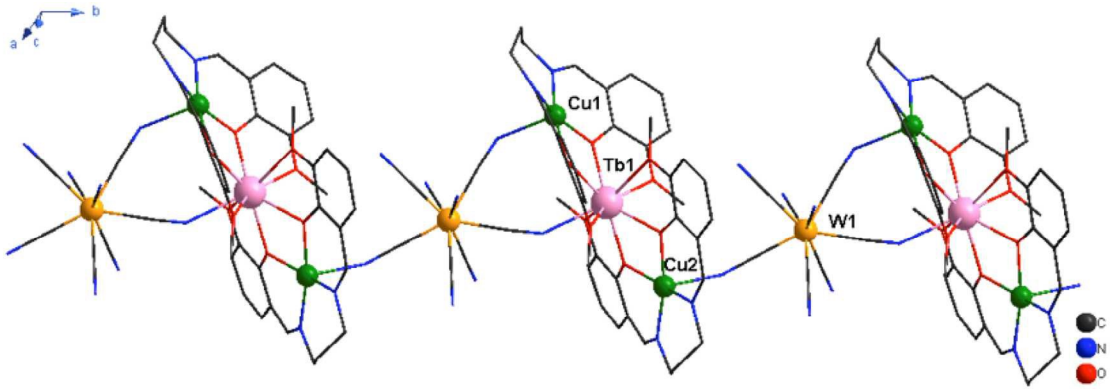

Figure 1. Fragment of the heterotrimetallic chain **6.**

Results and discussion

The reaction of $[\{Cu(L^1)\}_xLn(NO_3)_3]$ heterobimetallic complexes (H_2L^1 stands for H_2valpn and H_2valdp, x = 1, 2) with $(NHBu_3)_3[M(CN)_8]$ (M^V = Mo, W) afforded 1-D heterotrimetallic 3d-4f-4(5)d coordination polymers. Their topology appeared, however, to be dependent on the Schiff-base ligand involved. When H_2valpn Schiff-base pro-ligand was employed, an isomorphous series, gathered in **type 1** family, was obtained, having the general formula: $[\{Cu_2(valpn)_2Ln\}\{M(CN)_8\}]\cdot nH_2O\cdot mCH_3CN$ [Ln = La (**1**), Ce (**2**), Eu (**3**), Tb (**4**), Ho (**5**), M^V = Mo; Ln = Tb (**6**), Ho (**7**), M^V = W; m = 0, n =1 (**5**), 1.5 (**7**) and 2 (**1-4**, **6**); m = 1 (**5**)]. In the same reaction conditions, the use of the more rigid ligand H_2valdp gave rise to zigzag chains of formula $[\{Cu(valdp)Ln(H_2O)_4\}\{M(CN)_8\}]\cdot 2H_2O$ (**type 2**) [Ln = Gd (**8**), Tb (**9**), Dy (**10**); M = Mo; Ln = La (**11**), Gd (**12**), Tb (**13**), Dy (**14**); M = W]. With same ligand, but larger lanthanide(III) ions (La, Pr), a third chain motif, $[\{Cu_2(valdp)_2Ln(H_2O)_4\}\{Mo(CN)_8\}]\cdot nCH_3OH\cdot mCH_3CN$ (n = m = 0, Ln = La (**15**); n = m = 1, Pr (**16**)), was obtained, (**type 3**). The most remarkable aspect for these series of compounds is the diversity of connectivity found for the octacyanometallate(V) anions. Each $[M^V(CN)_8]^{3-}$ is linked to 3d-4f units by three of its CN^- for **type 1**, two for **type 2** and four for **type 3** (M = Mo, W).

Description of structures for compounds 1-7 (Type 1)

Compounds **1-6** are isomorphous and crystallize in the triclinic space group, *P-1*. The values of the cell parameters indicate that compound **7** is isomorphous with **type 1** series of compounds. They are also isomorphous with the Gd^{III} and Dy^{III} derivatives we have communicated earlier.[20a] The main bond distances and angles for compounds **1-6** are listed in Tables S2 and S3 in ESI. The **type 1** complexes differ by the number of the co-crystallized solvent molecules, thus only the structure for compound **6** will be described here.

The structure of **6** consists of heterotrimetallic chains and lattice solvent molecules (water and acetonitrile). The coordination polymer is assembled from an alternation of trinuclear phenoxo-bridged $\{Cu_2^{II}(valpn)_2Tb^{III}\}$ units and $\{M^V(CN)_8\}$ metallo-ligands inter-connected by three CN^- linkages. (Figure 1). The octacyanotungstate(V) unit exhibits a slightly distorted square antiprism geometry.[20a] It coordinates through two cyano groups to the Cu1 and Tb1 atoms of one 3d-4f unit, and to a second unit by a third cyano linked to the Cu2 center. The resulting 1-D structure parallels the crystallographic *b* axis.

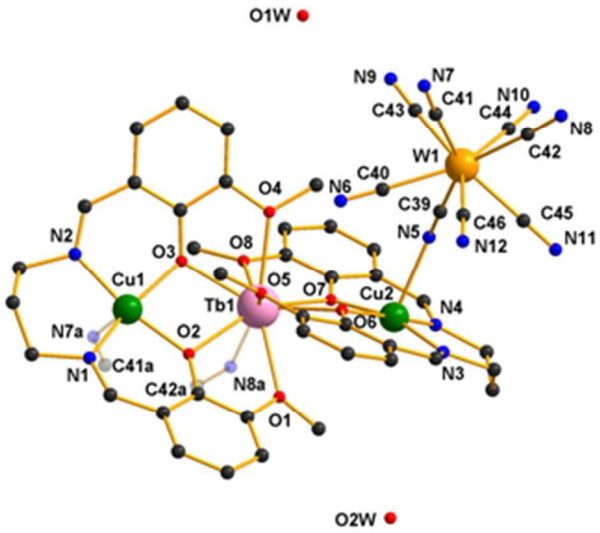

Figure 2. The asymmetric unit of **6** together with the atom labelling scheme (symmetry code [a] = x, -1+y, z).

Journal Name RSCPublishing

ARTICLE

The $\{Cu_2^{II}(valpn)_2Tb^{III}\}$ heterotrinuclear node is built from two $\{Cu^{II}(valpn)\}$ mononuclear units, connected through one terbium(III) ion, which is phenoxo-bridged to two copper(II) ions (Figure 2). The two crystallographically independent copper(II) cations are located in the inner compartments of the side-off ligand $valpn^{2-}$ and are five-coordinated, with a square-pyramidal geometry. The basal plane is formed by the N_2O_2 group of donor atoms belonging to the Schiff-base ligand and the apical coordination site of copper(II) atoms is occupied by one nitrogen atom from a cyano group. The Cu-N and Cu-O distances associated with the imino and phenoxo/methoxy groups of the Schiff-base ligand fall in the normal range.[18c,21,27a,32,33] For Cu-N bond lengths, the values vary between 1.970(5) and 1.981(5) Å and for the Cu-O bonds between 1.939(4) and 1.992(4) Å.

The copper(II) and terbium(III) ions are bridged by the phenoxo oxygen atoms of the compartmental ligand, the distance between the metal ions being 3.53 Å [Cu1···Tb1] and 3.52 Å [Cu2···Tb1]. The two phenoxo bridges are equivalent: the values of the Cu1-O2/O3-Tb1 and Cu2-O6/O7-Tb1 angles are 108.62(17)/108.65(16) and 109.46(17)/108.16(17)°, respectively. The rare-earth cation is nine-coordinated by eight oxygen atoms from phenoxo and methoxy groups and one nitrogen atom from a cyano group, in an approximately monocapped square antiprism geometry. The Tb-$O_{methoxy}$ bond lengths [2.478(5) - 2.585(4) Å] are slightly larger than Tb-$O_{phenoxo}$ distances [2.345(3) - 2.379(4) Å], all being comparable with those reported for similar molecular cores (in heterobi- or trimetallic complexes).[18c, 21, 27a, 32, 33]

The values of the distances associated to the cyano bridges are as follows: Cu1-$N7^a$ = 2.324(6) and Cu2-N5 = 2.330(6), Tb1-$N8^a$ = 2.462(6) Å (symmetry code: ^{a} = *x*, -1+*y*, *z*). Cyano-bridging ligands form bent angles with both 3d and 4f ions: Cu1-$N7^a$-$C41^a$ = 137.3(5)°, Cu2-N5-C39 = 142.2(5)°, Tb1-$N8^a$-$C42^a$ = 148.5(5)°. The terminal and bridging W-C-N fragments are almost linear, the corresponding angles ranging from 176.3(5) to 178.5(6)°. The intermetallic distances across the cyano bridges are: 5.20 [Cu1···$W1^a$], 5.31 [Cu2···W1] and 5.53 Å [Tb1···$W1^a$]. The neighboring chains are inter-connected and build supramolecular layers (parallel to the *ab* plane) through weak π-π stacking interactions employing the aromatic rings of the compartmental ligands (see Figure S1 in ESI).

Description of structures for compounds 8-14 (Type 2)

The crystal structures solved for compounds **10**-**14** and the cell parameters obtained for compounds **8** and **9** (see Experimental section) indicate that these complexes are isomorphous and crystallize in the monoclinic space group $P2_1$. The main bond distances and angles for compounds **10**-**14** are listed in Tables S4 and S5 in ESI. Their structures contain neutral $[\{Cu(valdp)Ln\}\{M(CN)_8\}]$ heterotrimetallic chains (M^V = Mo, W) and co-crystalized solvent molecules: water and acetonitrile. As a representative of this series, we will describe below $[\{Cu(valdp)Tb\}\{W(CN)_8\}]\cdot 2H_2O\cdot CH_3CN$ (**13**).

A view of the coordination polymer **13** is depicted in Figure 3a. The elementary unit contains one octacyanometallate(V) fragment coordinated, *via* one cyano ligand, to the copper atom of a $\{Cu^{II}Tb^{III}\}$ moiety (Figure 3b). The heterotrimetallic fragments are further linked through a second cyano group to the terbium(III) ion from an adjacent 3d-4f units. The $\{Cu^{II}Tb^{III}W^V\}$ trinuclear fragments are perpendicular to each other [W1-Cu1-$W1^a$ = 92.76°, symmetry code ^{a} = 1-*x*, -0.5+*y*, 1-*z*] resulting in a zigzag chain (Figure 3a).

The Cu^{II} ion is located into the N_2O_2 compartment of the Schiff-base and the rare-earth atom is placed in the outer O_2O_2' cavity of the ligand. The distances and angles related to the $\{Cu^{II}Tb^{III}\}$ unit have usual values.[34] For the square-pyramidal copper(II) ion, the basal plane is formed by the N_2O_2 set of donor atoms from the Schiff-base ligand, and the apical site is occupied by the $N9^a$ atom of a cyano group (symmetry code ^{a} = 1-*x*, -0.5+*y*, 1-*z*). The values of the bond lengths involving the N_2O_2 compartment of the Schiff-base are: Cu1-N1 = 1.916(18) and Cu1-N2 = 1.926(16) Å, Cu1-O2 = 1.927(11) and Cu1-O3 = 1.887(12) Å. The copper(II) cation is phenoxo-bridged to the rare-earth ion, the intramolecular Cu1···Tb1 distance being 3.39 Å. The values of the phenoxo bridge angles, Cu1-O2-Tb1 and Cu1-O3-Tb1, are 104.8(5) and 107.0(5)°, respectively. The terbium(III) ion is nine-coordinated, in a distorted monocapped square antiprism surrounding described by eight O atoms (four from compartmental ligand and four from aqua ~~molecules~~ ligands) and one nitrogen atom, N3, from the cyano bridge. The Tb-O bond lengths vary between 2.316(11) and 2.715(10) Å, the largest distances being associated to the methoxy oxygen.

The most relevant structural parameters comprising the cyano bridges are: Cu1-$N9^a$ = 2.504(14), Tb1-N3 = 2.482(14) Å, Cu1-$N9^a$-$C25^a$ = 146.3(2)° and Tb1-N3-C19 = 172.0(13)° (symmetry code ^{a} = 1-*x*, -0.5+*y*, 1-*z*). The cyano bridge angles with the copper(II) atom deviate from linearity, while the cyano group linked to the terbium(III) cation is quasi-linear. The intramolecular separations across the cyano bridges are: Cu1···$W1^a$ = 5.57 and Tb1···W1 = 5.80 Å.

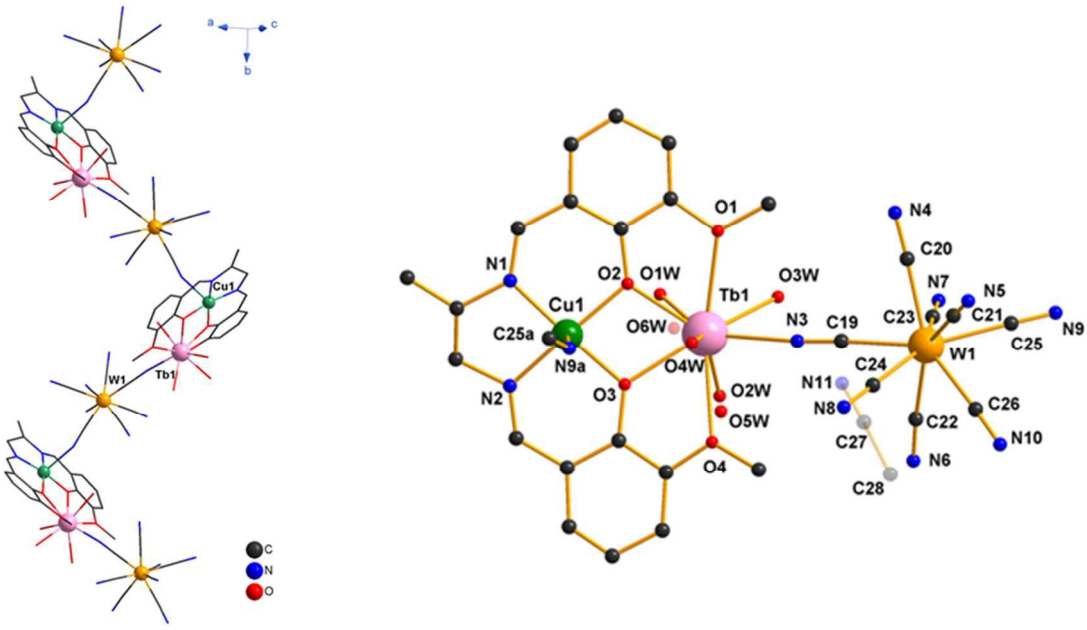

a b

Figure 3. (a) Fragment of the molecular structure of **13** showing the zigzag motif of the chain; (b) the asymmetric unit of **13** together with the atom labelling scheme ([a] = 1-*x*, -0.5+*y*, 1-*z*).

The inspection of the packing diagram showed the formation of three-dimensional supramolecular network through O···O and N···O type hydrogen bonds established between free cyano groups, crystallization water molecules and aqua ligands of terbium atoms belonging to neighboring heterotrimetallic chains (see Figure S2 in ESI). The distances associated with the hydrogen bonds span from 2.70 to 3.00 Å (see Table S6 in ESI). Neighboring chains are interconnected by hydrogen bonds, developing supramolecular layers in *ac* and *bc* plane. The closest W···W and Tb···Tb interchain distances (in *ac* plane) are equal (9.15 Å), while the closest W···Tb interchain separation, in *bc* plane, is 7.02 Å (see Figure S3 in ESI).

Description of structures for compounds 15 and 16 (Type 3)

Compound **15** crystallizes in the non-centrosymmetric orthorhombic space group $C222_1$, while compound **16** crystallizes in the monoclinic $P2_1/n$ space group. The main bond distances and angles for compounds **15** and **16** are listed in Table S7 and S8 in ESI. Both structures show a similar structural motif and consist of neutral $[\{Cu_2(valdp)_2Ln(H_2O)_4\}\{Mo(CN)_8\}]$ (Ln = La (**15**), Pr (**16**)) heterotrimetallic chains. We describe here the structure of **15**, the one of the Pr^{III} derivative (**16**) being shown in Figure S4 in ESI. The 1-D structures are assembled from trinuclear $\{Cu_2^{II}(valdp)_2La^{III}\}$ heterobimetallic units linked by $[Mo(CN)_8]^{3-}$ anions, which results in chains running along the crystallographic *c* axis. Half of the heterotrimetallic fragment $[\{Cu_2(valdp)_2La(H_2O)_4\}\{Mo(CN)_8\}]$ is crystallographically independent, two C_2 axis passing through La^{III} and Mo^{V} ions positions, in [1,0,0] and [0,1,0] directions, respectively (Figure S5 and S6).

In this coordination polymer, each $[Mo(CN)_8]^{3-}$ is bonded to two $\{Cu_2^{II}La^{III}\}$ units by four of its CN^- group coordinated respectively to La^{III} and to one of the Cu^{II} ions, each Cu^{II} of the trinuclear unit being linked to one metallo-ligand thus developing a 1-D array in which the two moieties alternate (Figure 4).

The copper(II)-lanthanum(III) trinuclear fragment results from two neutral mononuclear $\{Cu^{II}(valdp)\}$ units, which are coordinated to the La^{III} ions through the phenoxo-oxygen atoms, in a non-linear arrangement [the Cu1-La1-Cu2 angle is 129.9°] (see Figure 4). The distance between copper(II) and lanthanum(III) cations is 3.51 Å. The two assembling mononuclear units, $\{Cu^{II}(valdp)\}$, are twisted relative to each other, the dihedral angle between Cu1O2O3La1 and $Cu1^aO2^aO3^aLa1$ fragments being 54.5° (symmetry code: [a] = *x*, -*y*, -*z*).

The two copper(II) ions are located into the inner N_2O_2 pocket of the ligand, showing a distorted square-pyramidal geometry. For the two crystallographically equivalent copper atoms, the Cu-N bond lengths are 1.926(10) and 1.947(10) Å, and the Cu-O distances are 1.918(6) and 1.944(5) Å.

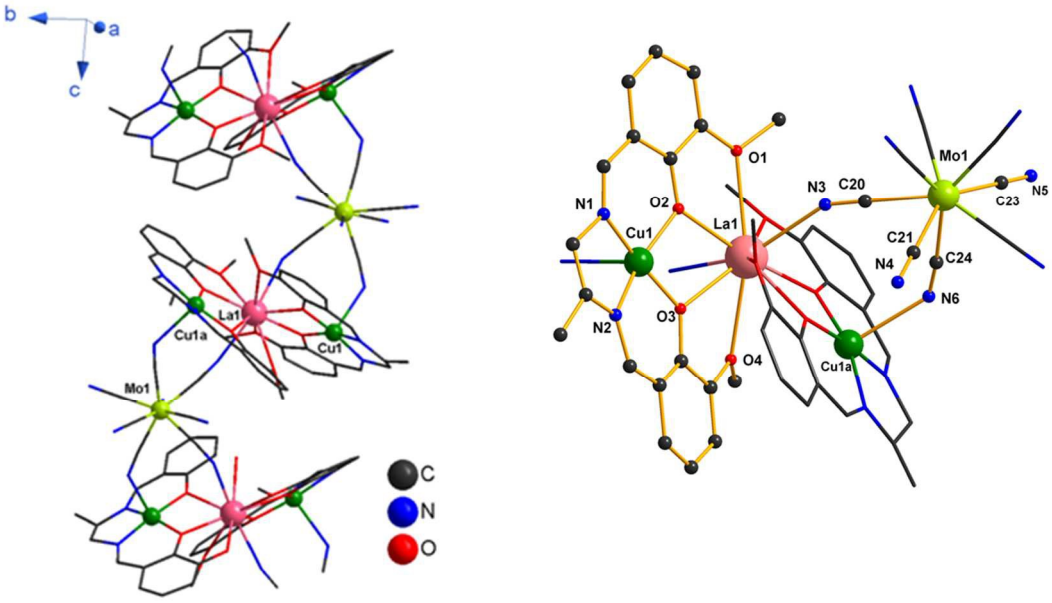

a b

Figure 4. (a) View along *c* axis of a fragment of the chain in **15**; (b) the heterotrimetallic assembling unit in **15** together with the atoms numbering (the molecular fragment generated by two-fold axis symmetry operations is represented with wires and sticks; symmetry code: [a] = *x*, -*y*, -*z*)

The apical position of the pyramid is occupied by one cyano group with Cu1-N6 = 2.485(1) Å.

Within the trinuclear $\{Cu_2^{II}(valdp)_2La^{III}\}$ moiety, the La^{III} cation is encapsulated between two outer $\{O_2O_2'\}$ compartments of the Schiff-base ligands. The lanthanum atom is ten-coordinated with eight oxygen atoms (four from methoxy groups and four from phenoxo bridges) and two nitrogen atoms from cyano bridges forming a distorted bicapped square antiprism polyhedra.

The La-O distances have common values, varying between 2.448(6) and 2.797(6) Å.[35,36] Two cyano groups of octacyanomolybdate(V) unit complete the coordination sphere of the lanthanum atom, the bond length being La1-N3 = 2.651(7) Å. The angles associated with the four cyano bridges deviate from linearity: Cu1[a]-N6-C24 = 132.2(3)°, La1-N3-C20 = 153.2(7)°. The distance between the copper(II) and molybdenum(V) ions across cyano bridges is Cu1[a]···Mo1 = 5.24 Å (symmetry code: [a] = *x*, -*y*, -*z*).

The lanthanum and molybdenum atoms are separated by the cyano bridge, with the distance La1···Mo1 = 5.78 Å. The chains are stacked in the crystal through C-H···π interaction (involving a methyl group of the lateral arm of the side-off ligand from one chain and a phenyl ring from the adjacent chain) building, a three-dimensional supramolecular network (see Figure S7 in ESI).

The comparative structural analysis of the three families of **type 1**, **type 2** and **type 3**, highlights the factors that influence the structural arrangement of the chains: (i) the nature of the side-off compartmental ligand, (ii) the coordination mode of the metallo-ligand, (iii) the nuclearity of the hetereobimetallic units and (iv) the ionic radii of the lanthanide(III) and/or second/third row transition cations. A slight modification of the lateral arm of the compartmental ligand induces significant structural changes (see Figure 5). This aspect was previously observed with $valen^{2-}$-based complexes, when discrete and 1-D heterotrimetallic structures were assembled.[20b]

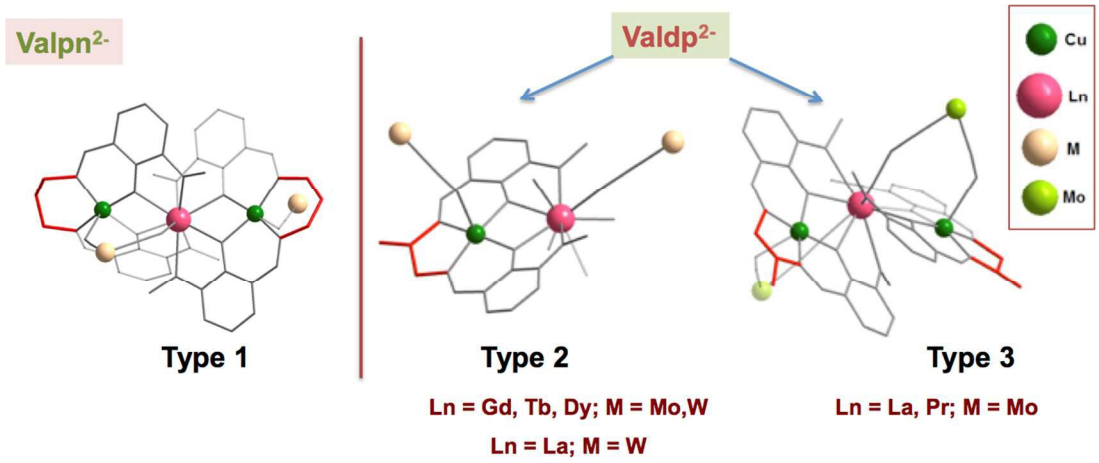

Figure 5. Schemes of the fragments of heterotrimetallic chains of **types 1** –**3**, illustrating the different structural arrangements of the 3d-4f assembling units influenced by the lateral arm of the compartmental ligand, the coordination modes of $[M(CN)_8]^{3-}$, and/or ionic radii of Ln^{III} ions.

The variation of the chain motif are closely related to the nuclearity of the 3d-4f heterobimetallic nodes and the coordination modes of $[M(CN)_8]^{3-}$ (M^V = Mo, W). Thus, a trinuclear $\{Cu_2^{II}Ln^{III}\}$ unit and a higher denticity (three or four) of the $[M(CN)_8]^{3-}$ anions formed **type 1** and **type 3** series, while a bis-monodentate coordination of octacyanometallates(V) unit is associated with binuclear $\{Cu^{II}Ln^{III}\}$ heterobimetallic moieties in **type 2** series.

For valdp^{2-} derivatives, **type 3** series is generated when larger lanthanide(III) ions are employed (Ln = La, Pr), the 3d-4f fragment being reorganized from binuclear into a trinuclear $\{Cu_2^{II}(valdp)_2Ln^{III}\}$ moiety. This chain rearrangement is produced only in the case of lighter 4d atom (Mo), the tungsten derivatives preserving the structural motif of the **type 2** series. Differences are observed also at supramolecular level. Thus, for **type 1** family, the chains are inter-connected through slipped-off π-π stacking interactions between two aromatic rings leading to supramolecular layers. For **type 3** family, the heterometallic chains also closely interact in the crystal and this might be attributed to C-H$\cdots\pi$ type interactions. In the case of isomorphous heterotrimetallic chains belonging to **type 2**, a three-dimensional supramolecular framework is constructed through hydrogen bonds involving terminal cyano ligands, coordinated aqua molecules and crystallization solvent molecules (water and acetonitrile).

Magnetic properties

Spin topologies

While all compounds exhibit 1-D structures enclosing 3d, 4f and 4/5d cations, the spin topology is different for each structural type. The particular spin topologies are represented schematically in Figure 6, showing the magnetic exchange pathways between the spin carriers.

For **type 1** family, the two phenoxo exchange pathways between copper(II) and lanthanide(III) ions, from the heterotrinuclear moiety, are equivalent (J_1) considering their structural similarity. The structural parameters of the cyano bridges between copper(II) and 4/5d ions are also similar and the coupling constants are expected to have very closed values ($J_2 = J_3$). The magnetic coupling between M^V and Ln^{III} ions through the cyano bridge is expected to be very weak (J_4).[19b, 37] The two copper(II) ions from the trinuclear moiety are separated by *ca*. 7 Å by the central Ln^{III} ions. A weak intramolecular next-neighbor interaction (J_1') between the the two copper(II) ions, *via* the Ln^{III} ion, is operative and was considered to model the overall magnetic behavior.[38]

Type 2 compounds consist of zigzag chains in which the copper(II) and lanthanide(III) ions interact through the phenoxo bridges within the binuclear assembling unit (J_1). Additional Cu^{II}-NC-M^V and Ln^{III}-NC-M^V pathways, characterized by J_2 and J_3, are also active within the chain. J_3 is anticipated to be very weak, according to previous reports.[19b, 37]

For **type 3** compounds, the topology of the spin centers is even more complicated than in **type 1** and **2** series, however the presence of the central diamagnetic lanthanum(III) cation simplifies the picture. The chain could be viewed as trinuclear {Cu1-NC-Mo1-CN-Cu1} moieties connected by diamagnetic La^{III} ions. The magnetic coupling scheme between the paramagnetic ions reduces to the cyano bridges and is described by J_2 in Figure 6. As in the case of **type 1** compounds, a weak next-neighbor magnetic interaction between the two copper(II) ions (distanced with *ca*. 6.36 Å) via the La^{III} ion (J_1' in Figure 6) must be considered.

The La^{III} derivatives of **type 1** (compound **1**) and for **type 2** (compound **11)** offer a good opportunity to evaluate the magnitude of the magnetic exchange interaction between copper(II) and molybdenum(V)/tungsten(V) ions across the cyano bridge.

Journal Name RSCPublishing

ARTICLE

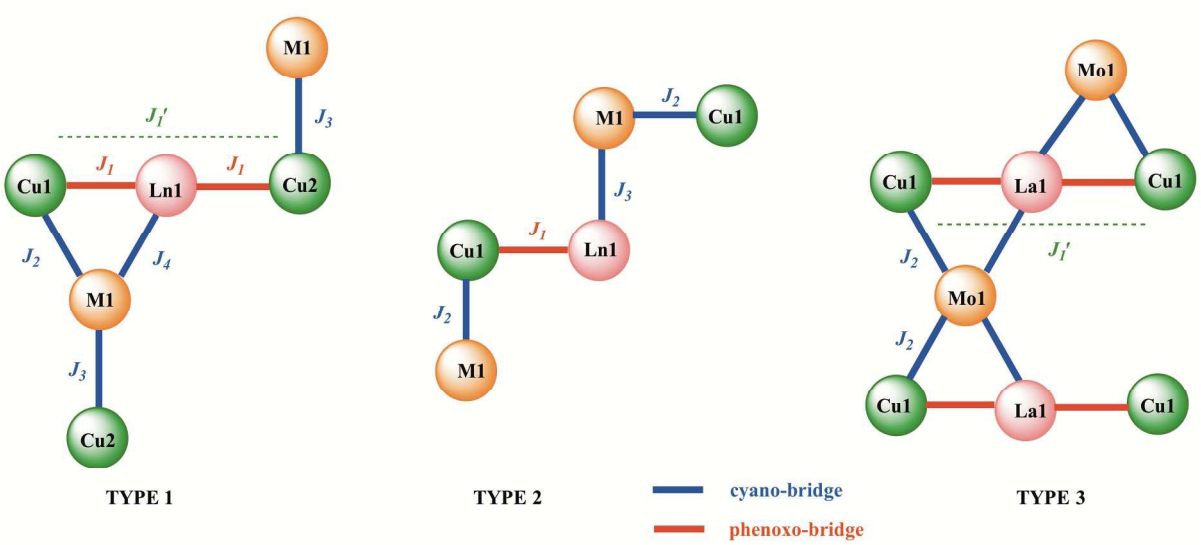

Figure 6. Spin topologies for the three families of compounds. For type 3, the represented situation applies for the diamagnetic La center.

Magnetic behavior for 1, 4 and 6 (type 1)

The thermal dependences of the $\chi_M T$ product for **4** and **6** are depicted in Figure 7.

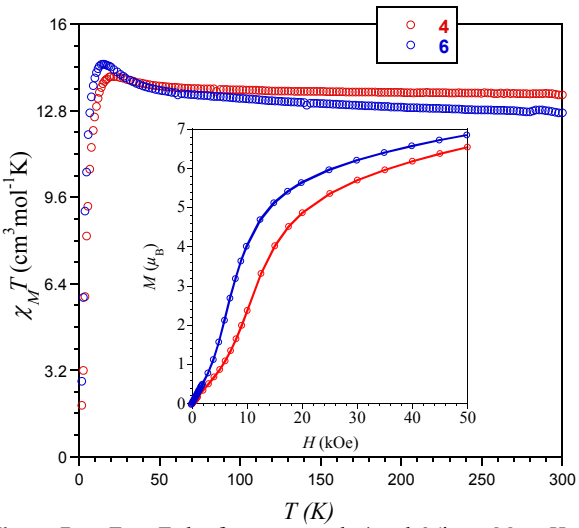

Figure 7. $\chi_M T$ *vs.* T plot for compounds 4 and 6 (inset M *vs.* H plot for 4 and 6).

At room temperature, the experimental values of the $\chi_M T$ product are 13.39 (**4**) and 12.72 (**6**) cm^{3}mol^{-1}K which correspond well to the expected value (12.94 cm^{3}mol^{-1}K) for copper(II) ($S_{Cu1} = S_{Cu2} = ½$, $g = 2.0$), molybdenum(V)/tungsten(V) ($S_{Mo1}/S_{W1} = ½$) and terbium(III) ion ($4f^8$, $J = 6$, $S = 3$, $L = 3$, $g_6 = 3/2$) non-interacting centers. The plots for **4** and **6** have similar shapes. As the temperature is reduced, $\chi_M T$ increases slowly, reaching a maximum of 14.06 (at *ca.* 20 K) for **4** and 14.50 cm^{3}mol^{-1}K (at *ca.* 15 K) for **6**. Below these temperatures, $\chi_M T$ drops to 1.9 (for **4**) and 2.8 cm^{3}mol^{-1}K (for **6**) at 2 K. The crystal field effect acting on the Ln^{III} center, supramolecular interactions (see Figure S4, SI) as well as the weak AF interaction between the two Cu^{II} cations across the Tb^{III} ions, within the trinuclear unit, may contribute to the decrease of the $\chi_M T$ plot, at low temperatures.[38] The ascendant curves result from the ferromagnetic interaction between the Cu^{II} and Tb^{III} ions. This magnetic behavior is a common feature for most of the phenoxo-bridged {Cu^{II}Tb^{III}} heterobimetallic complexes.[39] The field dependence of the magnetization M has a sigmoidal shape for both **4** and **6**, and the value at the high field is well below the saturation value. The origin of the S-shape of the $M = f(H)$ curve could be found in the strong magnetic anisotropy provided by Tb^{III} ions leading to anisotropic exchange interactions with the Cu^{II} centers[19a, 20a] and/or to the occurrence of an antiferromagnetic interaction (typically the next-neighbor Cu^{II}–Cu^{II} interaction). The critical field of the spin-flop phase transition has been determined from the maximum of the dM/dH derivative, being $H_c = 10$ kOe for compound **4** and 6 kOe for **6** (Figures S8 and S9 in ESI). The absence of saturation results from the magnetic anisotropy of the terbium(III) ions.

The ac magnetic measurements were performed for compounds **4** and **6** in order to investigate possible slow magnetization relaxation for these compounds. A frequency-dependent out-of-phase signal, χ_M", of the magnetic susceptibility was observed only in the presence of an applied DC fields. The results obtained for H_{DC} = 3 kOe are shown in Figure 8.

For compound **4** (Mo), the maximum exhibited by χ_M" is shifted towards higher temperature when the measuring frequency is increased; for ν = 1490 Hz the blocking temperature is 2.8 K (Figure 8 a). An evaluation of the effective energy barrier for the magnetization reversal and the pre-exponential parameters τ_0 associated to the χ_M" signals have been deduced from the plot of $\ln\tau = f(1/T_B)$ where τ is the relaxation time for a given frequency, *i.e.* $(2\pi\nu)^{-1}$, and T_B the blocking temperature (*i.e.,* the T of the maxima of χ_M" for this frequency). Fitting the Arrhenius law $\tau = \tau_0\exp(U_{eff}/k_BT)$ to the data points (inset Figure 8 a) lead to $\tau_0 = 5.5\cdot10^{-7}$ s and U_{eff}/k_BT = 20.5 K.

For compound **6**, the relaxation of the magnetization is fast and the maxima of the out-of-phase susceptibilities are not seen above 2 K, even under a DC magnetic field (Figure 8 b). This tendency was also found in the case of the isomorphous $\{Cu^{II}Dy^{III}W^{V}\}$ complex,[20a] for which the χ_M" signals (and maxima) are observed at lower temperatures than the molybdenum(V) analogues. Thus, for compound **6**, under the assumption that there is only one relaxation process characterized by the pre-exponential relaxation time (τ_0) and an activation energy (U_{eff}), and considering that the adiabatic susceptibility is zero, these parameters can be evaluated with Equation (1).[40] In this expression ω is the experimental ac field frequency (where $\omega = 2\pi\upsilon$ with the ac field frequency υ), and χ_M' and χ_M" are the values taken by the in- and out-of-phase component for a given T. The values obtained for U_{eff} and τ_0 are 15.1 K and 1.5 10^{-7} s, respectively.

$$\ln(\chi_M''/\chi_M') = \ln(\omega\tau_0)+U_{eff}/k_BT \qquad (1)$$

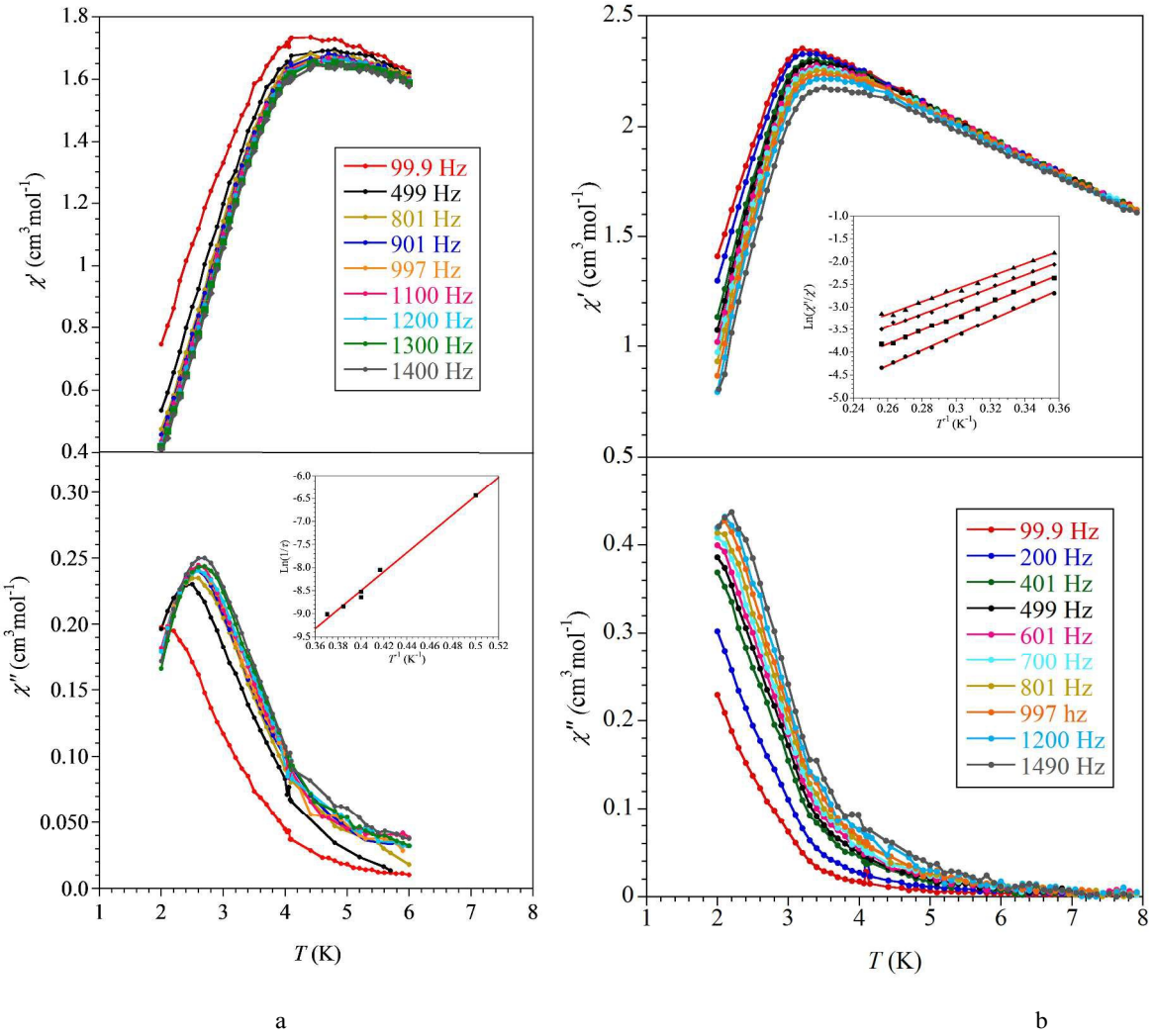

Figure 8. Thermal dependence of the in-phase (up) and out-of-phase (bottom) magnetic susceptibility, χ_M' and χ_M" for the compounds **4** (a) and **6** (b) in H_{DC} = 3000 Oe applied DC field. Inset: (a) Arrhenius plot for **4**; (b) natural logarithm of the χ''/χ' ratio vs. $1/T$ under a DC magnetic applied field of 3000 Oe and a 3 Oe oscillating field at four different frequencies. Solid lines represents the best fits.

Journal Name RSCPublishing

ARTICLE

The anisotropy and the dynamic magnetic properties found for the Tb^{III} derivatives, **4** and **6**, differ from that of the Dy^{III} homologue.[20a] For the latter, the slow relaxation of the magnetization in the zero DC field was observed, while for the terbium(III) compounds it was only found under applied DC field. This could result from the electronic structure of the non-Kramers ion of Tb^{III} ($4f^8$, $^7F_6$ ground state), which is more exposed to the effects of the ligand field than the dysprosium(III) one (a Kramers ion, $4f^9$ and $^6H_{15/2}$).[26a,c] Recent DFT calculations performed on the isostructural phenoxo-bridged $\{Cu^{II}Ln^{III}\}$ binuclear SMM's complexes (Ln^{III} = Tb, Dy) revealed that the anisotropy and the calculated energy splitting between the ground and the first excited sub-levels for Dy^{III} derivative is higher than in the Tb^{III} case.[39d]

Based on the chain structures for **4** and **6**, the slow relaxation of the magnetization might be ascribed to a SCM behavior having its origin in the anisotropy of the Ln^{III} ion. In order to confirm that magnetic interactions are propagated along the 1-D spin arrays by the cyanometallate units we considered the La^{III} derivative (**1**). Complex **1** was used to estimate the nature and the magnitude of the magnetic coupling between Cu^{II} and Mo^{V} ions *via* cyano bridge.

The thermal dependence of the $\chi_M T$ for compound **1** is represented in Figure 9 (χ_M is the magnetic susceptibility per $\{Cu^{II}_2La^{III}Mo^{V}\}$ unit). The value of $\chi_M T$ at room temperature is 1.27 $cm^3mol^{-1}K$, which is slightly above the estimated value for two copper(II) (S_{Cu} = ½) and one molybdenum(V) (S_{Mo} = ½) magnetically diluted ions (1.12 $cm^3mol^{-1}K$, assuming g = 2.00). By decreasing the temperature, $\chi_M T$ remains practically constant down to 30 K, and then it decreases abruptly to reach 0.34 $cm^3mol^{-1}K$, at 2 K. This is the result of a dominant antiferromagnetic behavior as confirmed by the fit of χ_M^{-1} *vs.* T plot, that follow the Curie-Weiss law: C = 1.21 cm^3Kmol^{-1} and θ = -1.09 K, where C and θ are the Curie and Weiss constant, respectively (inset Figure 9). The magnetic properties are consistent with the isomorphous W^{V} derivative.[20a] The magnetic behavior of **1** is mainly the result of the intramolecular magnetic interactions within $\{Cu_2^{II}Mo^{V}\}$ trimers, in which the two cyano-based exchange pathways are considered equivalent, due to the close values of the cyano angles [Cu1-N7-C41 =143.05 and Cu2^a-N5-C39 = 142.1(5)^o]. The magnetic data for compound **1** were simulated using the isotropic spin Hamiltonian for a linear Cu^{II}-M^{V}-Cu^{II} system (Equation (2)) to model the trinuclear $Cu_2^{II}Mo^{V}$ moiety with $S_1 = S_2 = S_{Cu} = S_{Mo} = 1/2$:

$$\boldsymbol{H} = -2J(\boldsymbol{S}_1\boldsymbol{S}_2 - \boldsymbol{S}_2\boldsymbol{S}_3) \qquad (2)$$

Equation 3 corresponds to the expression of the van Vleck equation:

$$\chi_{M(trimer)} = \frac{Ng^2\beta^2}{4kT} \cdot \frac{1+\exp\left(\frac{2J}{kT}\right)+10\exp\left(\frac{3J}{kT}\right)}{1+\exp\left(\frac{2J}{kT}\right)+2\exp\left(\frac{3J}{kT}\right)} \qquad (3)$$

where J is the coupling constants between copper(II) and molybdenum(V) ions through the cyano bridges, g is the Landé factor, k_B is the Boltzmann constant and β is the Bohr magneton. In order to assess the possible interference of weak intra- and intermolecular interactions, the corresponding interaction (zJ') was considered within the mean-field approximation (Eq. 4):

$$\chi_m = \frac{\chi_{M(trimer)}}{1-\frac{zJ'\chi_{M(trimer)}}{Ng^2\beta^2}} \qquad (4)$$

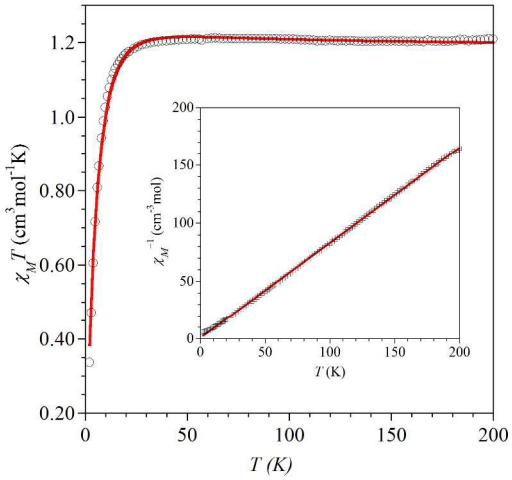

Figure 9. $\chi_M T$ *vs.* T plot for compound 1. Inset χ_M^{-1} *vs* T representation for compound 1 ((o) experimental; (–) best-fit curve through eq. (4) (see text).

Least-squares fit to the data led to the following results: g = 2.05, J = + 7.7 cm^{-1} and zJ' = -4.5 cm^{-1}, R = 22.1 × 10^{-4} for **1**. R is the agreement factor defined as $\sum_i[(\chi_M T)_{obs} - (\chi_M T)_{calc}]^2 / \sum_i[(\chi_M T)_{obs}]^2$.

The best fit results emphasize both ferro- and antiferromagnetic interactions. The ferromagnetic nature of the magnetic coupling between Cu^{II} and Mo^{V} through the cyano bridge was also evidenced for the isomorphous Gd^{III} and Dy^{III} derivatives.[20a]

Journal Name RSCPublishing

ARTICLE

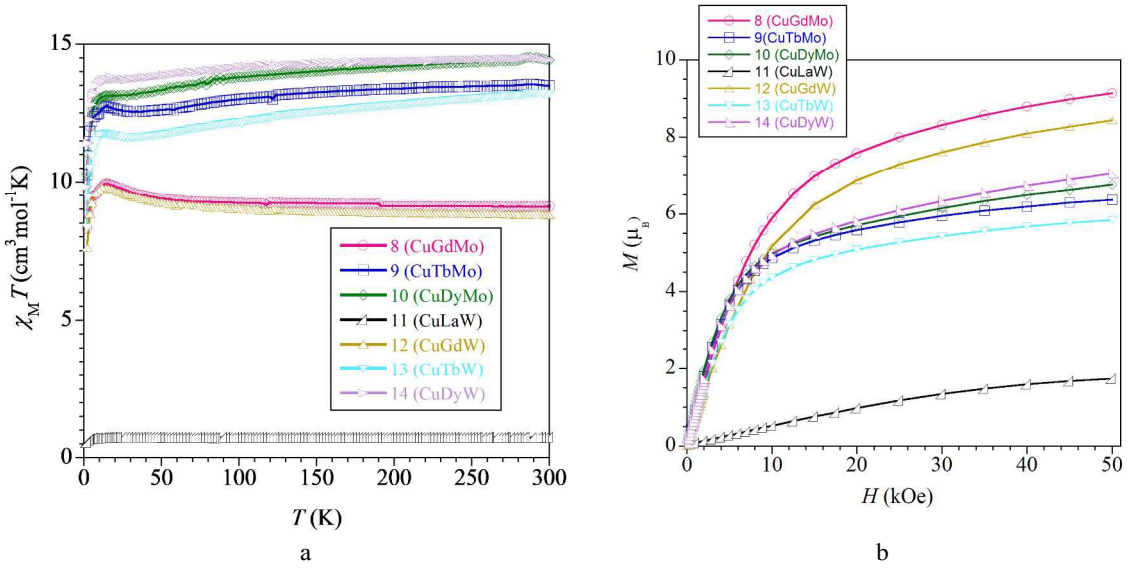

Figure 10. (a) Temperature dependence of the $\chi_M T$ product for **8-14** at 1000 Oe; (b) the field dependence of the magnetization for compounds **8-14.** Solid lines is an eye-guide.

The AF interaction results from both supramolecular interactions (see Figure S1 in ESI) and the weak coupling between the two opposite copper(II) ions via the Ln^{III} ion, within the trinuclear moiety (J'_1). However, while the mathematical fit is fine, the obtained values for both J and zJ' reveal that our model is not adapted to analyze properly these data. Indeed the resulting exchange parameters are too large[41] and their ratio does not satisfy with the mean-field approximation (i.e. zJ' < 10% of J).[42] This supports the assumption that the magnetic behavior for **1** corresponds to a spin-chain.

Magnetic properties of 8-14 (type 2)

The thermal dependences of $\chi_M T$ for compounds **8-14** are illustrated in Figure 10 a).

First we will focus on the chains containing isotropic Gd^{III} ions, namely $\{(Cu^{II}(valdp)Gd^{III}Mo^{V}\}$ (**8**) and $\{(Cu^{II}(valdp)Gd^{III}W^{V}\}$ (**12**). The $\chi_M T$ product is equal to 9.11 (**8**) and 8.9 cm^3 K mol^{-1} (**12**) at room temperature, being slightly lower than the calculated value of 9.45 cm^3 K mol^{-1} for uncoupled spin carriers i.e., one Gd^{III} (S = 7/2, g = 2.0), one Mo^{V}/W^{V} ($S_{Mo/W}$ = ½, g = 2.0) and one Cu^{II} (S_{Cu} = ½, g = 2.2). Upon cooling, the value of $\chi_M T$ remains constant down to *ca.* 50 K, then increases reaching a maximum of 10 cm^{3}mol^{-1}K at 15 K (compound **8**), and 9.80 cm^{3}mol^{-1}K at 12 K (compound **12**). At lower temperatures, both curves sharply decrease (8.31 for **8** and 7.61 cm^{3}mol^{-1}K for **12**, at 2 K) most likely due to the antiferromagnetic inter-chain interactions through the extended hydrogen-bond network (see Figure S2 and S3 in ESI). The magnetic behavior of the two Gd^{III} derivatives is very similar and can be explained by the ferromagnetic interactions usually detected between Cu^{II} and Gd^{III} centers.[39a,e,43] In Figure 10 b is represented the field dependence of the magnetization, at 2 K (for both gadolinium(III) derivatives) revealing that M is not saturated at 5 T. This is a typical behavior for ferromagnetic systems with next-neighbor antiferromagnetic interactions.[38b]

All the other complexes, except compound **11**, exhibit similar plot shapes as compounds **8** and **12** (see Figure 10). In order to compare the magnetic behavior of **type 1** (compounds **4** and **6** previously discussed) and **type 2** families, we will further discuss only the magnetic properties of the terbium(III) derivatives of **type 2**, namely compounds **9** and **13**. The room temperature values of the $\chi_M T$ product of **9** (13.50 cm^3 K mol^{-1}) and **13** (13.20 cm^3 K mol^{-1}) are consistent with the expected value of 12.65 cm^3 K mol^{-1} for isolated spin carriers, that is, one Tb^{III} ($4f^8$,J = 6, S = 3, L = 3, g_6= 3/2), one Mo^{V}/W^{V} (S_W = ½, g = 2.0), and one Cu^{II} (S_{Cu} = ½, g = 2.2). Upon cooling, the value of the $\chi_M T$ product decreases to 12.5 cm^{3}mol^{-1}K for compound **9** and 11.62 cm^{3}mol^{-1}K for compound **13**, at 35 K. This behavior is due, in both cases, to the depopulation of the M_J levels of the $^7F_6$ state.[44] Between 35 and 15 K, an increase of the value of the $\chi_M T$ product is observed (12.75 for compound **9** and 11.75 cm^3 K mol^{-1} for compound **13**) indicating a ferromagnetic interaction. Finally, below 15 K, $\chi_M T$ sharply decreased reaching, at 1.8 K, the value of 10.26 (for compound **9**) and 8.32 cm^3 K mol^{-1} (for compound **13**).

The drop of the $\chi_M T$ plot, at low temperatures, is most likely a result of the magnetic anisotropy, usually observed for these systems, and/or AF inter-chain interactions mediated by hydrogen bonds (see Figure S2 and S3 in ESI). For both compounds, the field dependence of the magnetization *M* was measured at 2 K (see Figure 10 b) showing that the saturation is not reached at 5 T.

AC magnetic measurements were also performed on polycrystalline samples of compounds **9** and **13,** under 0 DC field and under a DC field of 1000 Oe. In both cases, no maxima were observed on the in-phase or out-of-phase susceptibility components in these conditions (Figures S10 and S11 in ESI). This aspect is rather surprising taking into account our recent report including the $[\{W(CN)_8\}Cu(valen)Tb(OH_2)_4]\cdot CH_3CN\cdot H_2O$ heterotrimetallic chain, isostructural with compound **13**, that shows a SCM behavior with a significant value of the barrier energy (U_{eff}/k_BT= 53.9 K).[20b]

Compound **11** contains the diamagnetic La^{III} ion and could provide more insights into the nature of magnetic interaction between Cu^{II} and W^{V}, through the cyano bridge. The temperature dependence of $\chi_M T$ product of compound **11** was measured at 1000 Oe (Figure 10 a). The value of the $\chi_M T$ product is 0.70 $cm^3mol^{-1}K$ at room temperature, and corresponds to the calculated value of 0.83 cm^3 K mol^{-1} for the uncoupled spin carriers of one W^{V} (S_W = ½, *g* = 2.0) and one Cu^{II} (S_{Cu} = ½, *g* = 2.2). Upon cooling, the $\chi_M T$ curve remained almost constant down to 15 K then sharply decreased to reach 0.6 $cm^3mol^{-1}K$ at 2 K. This behavior indicates that the magnetic interaction between Cu^{II} and W^{V} centers are very weak or negligible, while the low temperature behavior is most probably due to the antiferromagnetic interchain interactions mediated by the hydrogen bonds (see Figures S2 and S3 in ESI). The field dependence of the magnetization *M* for compound **11** was measured at 2 K showing that saturation is not reached at 5 T and *M* tends to 2 μ_B as expected for two spins ½ either independent or in ferromagnetic interaction.

Magnetic properties of the compound 15 (type 3)

The temperature dependence of the $\chi_M T$ product of compound **15**, measured at 1000 Oe, is represented in Figure S12 in ESI. The $\chi_M T$ product is 0.76 $cm^3mol^{-1}K$ at room temperature, in agreement with the calculated value of 0.86 $cm^3mol^{-1}K$ for the uncoupled spin carriers: one Mo^{V} (S_{Mo} = ½, *g* = 2.0) and one Cu^{II} ions (S_{Cu} = ½, *g* = 2.2). Upon cooling, the $\chi_M T$ value increases to 0.90 $cm^3mol^{-1}K$ at 20 K, then the curve sharply decreases, reaching a value of $\chi_M T$ of 0.70 cm^3 K mol^{-1}, at 2 K. This magnetic behavior indicates ferromagnetic interaction between Cu^{II} and Mo^{V} ions, while the low temperature behavior is the result of the antiferromagnetic inter-chain interactions (see Figure S12 in ESI). This behavior could not be properly modeled by a simple three spin equation.

Conclusions

The distinct structural features, obtained for three series of 3d-4f-4(5)d heterotrimetallic chains compounds reported herein, confirm the role played by several chemical parameters on the resulting association scheme. In strictly same reaction conditions, the structural characteristics of the compartmental ligand (H_2valpn versus H_2valdp in present examples), the ionic radii of the 4f and that 4(5)d ions are factors that may influence the actual nuclearity of the 3d-4f unit involved, the coordination mode of the $[M^{V}(CN)_8]^{3-}$ anions, and, in turn, the resulting supramolecular arrangement of the coordination compound.
Herein, a minor modification of the lateral chain of the Schiff-base ligand is accompanied by a change of nuclearity of the 3d-4f unit and coordination mode of the metallo-ligand. This is illustrated by trinuclear $\{Cu_2^{II}Ln^{III}\}$ moiety found with the $valpn^{2-}$-type ligand (in **type 1**) whereas, in the same conditions, binuclear $\{Cu^{II}Ln^{III}\}$ units have been found with the $valdp^{2-}$ ligand (in **type 2**). This effects the coordination preference of the $[M^{V}(CN)_8]^{3-}$ spacer which exhibits tri-connecting or bi-connecting preferences, respectively.

The size of the Ln^{III} ions may also influence the assembling scheme but this appears dependent on the Schiff-based ligands. Hence, while the size of the Ln^{III} ions has no effect in the case of $valpn^{2-}$ ligand (**type 1**), larger Ln^{III} ions alter the supramolecular organisation for $valdp^{2-}$-based derivatives. Thus, a reorganization of the $\{Cu^{II}Ln^{III}\}$ node from bi- (**type 1**) to tri-nuclear units (**type 3**), with tetra-connecting $\{Mo^{V}(CN)_8\}$ spacers, is found for La^{III} and Pr^{III} ions.

From **type 1** family, the Tb^{III} derivatives (compounds **4** and **6**) showed slow relaxation of the magnetization in applied DC field (H_{DC} = 3000 Oe). In the same family, the analysis of the magnetic properties of the La^{III} derivative (compound **1**) revealed a weak F coupling assigned to the exchange interaction between Cu^{II} and Mo^{V} ions through the cyano bridge, most probably overwhelmed by next-neighbor intramolecular and intermolecular AF interactions. A similar magnetic behavior was observed for La^{III} complex (compound **15**) belonging to **type 3** series of compounds. The magnetic properties of the heterotrimetallic chains with a zigzag topology belonging to **type 2** family, indicate, in all cases, a predominant ferromagnetic interaction (due to the magnetic coupling between Cu^{II} and Ln^{III} ions through phenoxo bridge within the 3d-4f assembling unit).

The examples of heterotrimetallic complexes presented in this paper bring us closer to a better understanding of their magnetic properties in correlation with the structural peculiarities. Further results on this chemistry will be presented in subsequent papers.

Acknowledgements

Financial support from the UEFISCDI (grant PNII-ID-PCCE-2011–2-0050) is gratefully acknowledged.

Notes and references

[a] Coordination and Supramolecular Chemistry Laboratory, Institute of Physical Chemistry "Ilie Murgulescu", Romanian Academy, Splaiul Independentei 202, 060021 Bucharest, Romania. E-mail: diana.visinescu@gmail.com
[b] Inorganic Chemistry Laboratory, Faculty of Chemistry, University of Bucharest, Str. Dumbrava Rosie, nr. 23, 020464 Bucharest, Romania. E-mail: marius.andruh@dnt.ro
[c] CNRS; LCC (Laboratoire de Chimie de Coordination); 205, route de Narbonne, F-31077 Toulouse, France. E-mail: sutter@lcc-toulouse.fr
[d] Université de Toulouse; UPS, INPT; LCC; F-31077 Toulouse, France

† Electronic Supplementary Information (ESI) available: IR spectra discussion, crystal packing for compound **6** (Figure S1), for compound **13** (Figure S2 and S3), molecular structure for compound **16** (Figure S4), view of the helicoidal motif in compound **15** (Figures S5 and S6), crystal packing for compound **15** (Figure S7), plots of *M* and d*M*/d*H* *vs*. *H* plot for compounds **4** and **6** (Figures S8 and S9), χ_M" *vs*. *T* for compound **9** (Figure S10) and χ_M' and χ_M" *vs*. *T* for compound **13** (Figure S11), χ_M *vs*. *T* (Inset *M* *vs*. *H*) for compound **15** (Figure S12), crystal data and detail of the crystal determinations for compound **16** (Table S1), the main bond distances and angles values for compounds **1-6** (Table S2 and S3), **10-14** (Table S4 and S5) and **15-16** (Table S7 and S8), selected hydrogen-bond lengths for compounds **10-14** (Table S6). See DOI: 10.1039/b000000x/

1 (a) O. M. Yaghi, M. O'Keeffe, N. W. Ockwig, H. K. Chae, M. Eddaoudi, J. Kim, *Nature*, 2003, **423**, 705; (b) K. Sumida, D. L. Rogow, J. A. Mason, T. M. McDonald, E. D. Bloch, Z. R. Herm, T.-H. Bae, J. R. Long, *Chem. Rev.*, 2012, **112**, 724; (c) M. P. Suh, H. J. Park, T. K. Prasad, D.-W. Lim, *Chem. Rev.*, 2012, **112**, 782.
2 (a) A. M. Kirillov, M. V. Kirillova, A. J. L. Pombeiro, *Coordin. Chem. Rev.*, 2012, **256**, 2741; (b) J. García-Antón; R. Bofill, L. Escriche, A. Llobet, S. Xavier, *Eur. J. Inorg. Chem.*, 2012, 4775; (c) X. Liu, F. Wang, *Coordin. Chem. Rev.*, 2012, **256**, 1115; (d) B. G. Cooper, J. Napoline Wesley, C. M. Thomas, *Catal. Rev.*, 2012, **54**, 1.
3 (a) M. W. Cooke, D. Chartrand, G. S. Hanan, *Coordin. Chem. Rev.*, 2008, **252**, 903; (b) A. Barbieri, G. Accorsi, N. Armaroli, *Chem. Commun.*, 2008, 2185; (c) M. D. Ward, *Coordin. Chem. Rev.*, 2007, **251**, 1663; (d) Y. Cui, Y. Yue, Q. Guodong, B. Chen, *Chem. Rev.*, 2012, **112**, 1128.
4 (a) J. S. Miller, *Chem. Soc. Rev.*, 2011, **40**, 3266; (b) P. Dechambenoit, J. R. Long, *Chem. Soc. Rev.,* 2011, **40**, 3249; (c) N. Roques, V. Mugnaini, J. Veciana, *Top. Curr. Chem.*, 2010, **293**, 207.
5 (a) C. L. M. Pereira, E. F. Pedroso, A. C. Doriguetto, J. A. Ellena, K. Boubekeur, Y. Filali, Y. Journaux, M. A. Novak, H. O. Stumpf, *Dalton Trans.*, 2011**,** **40**, 746; (b) S. Wang, X.-H. Ding, J.-L. Zuo, X.-Z. You, W. Huang, *Coordin. Chem. Rev.*, 2011, **255**, 1713.
6 (a) P. Chaudhuri, *Coordin. Chem. Rev.*, 2003, **243**, 1437; (b) C. Paraschiv, M. Andruh, Y. Journaux, Z. Žak, N. Kyritsakasd, L. Ricard, *J. Mater. Chem.*, 2006, **16**, 2660.
7 (a) S. Ferlay, T. Mallah, R. Ouahes, P. Veillet, M. Verdaguer, *Nature*, 1995, **378**, 701; (b) O. Hatlevik, W. E. Buschmann, J. Zhang, J. L. Manson, J. S. Miller, *Adv. Mater.*, 1999, **11**, 914; (c) W. R. Entley, G. Girolami, *Science*, 1995, **268**, 397; (d) S. M. Holmes, S. G. Girolami, *J. Am. Chem. Soc.*, 1999, **121**, 5593.
8 (a) T. Glasser, *Chem. Commun.*, 2011, **47**, 116; (b) R. Sessoli, A. Powell, *Coordin. Chem. Rev.*, 2009, **253**, 2328; (c) H. Miyasaka, M. Julve, M. Yamashita, R. Clérac, *Inorg. Chem.*, 2009, **48**, 3420; (d) H.-L. Sun, Z.-M. Wang, S. Gao, *Coordin. Chem. Rev.*, 2010, **254**, 1081; (e) W.-X. Zhang, R. Ishikawa, B. Breedlove, M. Yamashita, *RSC Adv.*, 2013, **3**, 3772.
9 (a) R. Winpenny, *Angew. Chem. Int. Ed.*, 2008, **47**, 7992; (b) F. Troiani, M. Affronte, *Chem. Soc. Rev.*, 2011, **40**, 3119; (c) G. Aromi, D. Aguilà, P. Gamez, F. Luis, O. Roubeau, *Chem. Soc. Rev.*, 2012, **41**, 537.
10 M. Verdaguer, A. Bleuzen, V. Marvaud, J. Vaissermann, M. Seuleiman, C. Desplanches, A. Scuiller, C. Train, R. Garde, G. Gelly, C. Lomenech, I. Rosenman, P. Veillet, C. Cartier, F. Villain, *Coordin. Chem. Rev.*, 1999, **190-192**, 1023.
11 C. N. Verani, T. Weyhermüller, E. Rentschler, E. Bill, P. Chaudhuri, *Chem. Commun.*, 1998, 2475.
12 (a) D. S. Nesterov, V. N. Kokozay, B. W. Skelton, *Eur. J. Inorg. Chem.*, 2009, 5469; (b) D. S. Nesterov, V. N. Kokozay, V. V. Dyakonenko, O. V. Shishkin, J. Jezierska, A. Ozarowski, A. M. Kirillov, M. N. Kopylovich, A. J. L. Pombeiro, *Chem. Commun.*, 2006, 4605; (c) D. S. Nesterov, C. Graiff, A. Tiripicchio, A. J. L. Pombeiro, *CrystEngComm*, 2011, **13**, 5348; (d) D. S. Nesterov, V. G. Makhankova, O. Yu. Vassilyeva, N. Kokozay, L. A. Kovbasyuk, B. W. Skelton, J. Jezierska, *Inorg. Chem.*, 2004, **43**, 7868.
13 (a) H.-Z. Kou, B. C. Zhou, S. Gao, R.-J. Wang, *Angew. Chem. Int. Ed.*, 2003, **42**, 3288; (b) H. - Z. Kou, B. C. Zhou, R.-J. Wang, *Inorg. Chem.*, 2003, **42**, 7658; (c) H.-Z. Kou, K.-Q. Hu, H.-Y. Zhao, J. Tang, A.-L. Cui, *Chem. Commun.*, 2010, **46**, 6533.
14 (a) T. Shiga, H. Ohkawa, S. Kitagawa, M. Ohba., *J. Am. Chem. Soc.*, 2006, **116**, 16426; (b) X.-J. Song, Z.-C. Zhang, Y.-L. Xu, J. Wang, H.-B. Zhou, Y. Song, *Dalton Trans.*, 2013, **42**, 9505;(c) T. Shiga, A. Mishima, K. Sugimoto, H. Okawa, H. Oshio, M. Ohba, *Eur. J. Inorg. Chem.*, 2012, 2784.
15 M. Andruh, *Chem. Commun.*, 2011, **47**, 3025.
16 (a) D. Visinescu, J.-P. Sutter, C. Ruiz-Pérez, M. Andruh, *Inorg. Chim. Acta*, 2006, **359**, 433; (b) H. Wang, L.-F. Zhang, Z.-H. Ni, W.-F. Zhong, L.-J. Tian, J. Jiang, *Cryst. Grow. Des.*, 2010, **10**, 4231.
17 M. A. Palacios, A. J. Mota, J. Ruiz, M. M. Hanninen, R. Sillanpaa, E. Colacio, *Inorg. Chem*., 2012, **51**, 7010.
18 (a) R. Gheorghe, M. Andruh, J.-P. Costes, B. Donnadieu, *Chem. Commun.*, 2006, 2778; (b) R. Gheorghe, P. Cucos, M. Andruh, J.-P. Costes, B. Donnadieu, S. Shova, *Chem. Eur. J.*, 2003, **12**, 187; (c) R. Gheorghe, A. M. Madalan, J.-P. Costes, W. Wernsdorfer, M. Andruh, *Dalton Trans.*, 2010, **49**, 4734.
19 (a) S. Dhers, J.-P. Costes, P. Guionneau, C. Paulsen, L. Vendier, J.-P. Sutter, *Chem. Commun.*, 2015, **51**, 7875; (b) J.-P. Sutter, S. Dhers, R. Rajamani, S. Ramasesha, J.-P. Costes, C. Duhayon, L. Vendier, *Inorg. Chem.*, 2009, **48**, 5820; (b) S. Dhers, S. Sahoo, J.-P. Costes, C. Duhayon, S. Ramasesha, J.-P. Sutter, *CrystEngComm*, 2009, **11**, 2078; (c) J.-P. Sutter, S. Dhers, J.-P. Costes, C. Duhayon, *C. R. Chem*., 2008, **11**, 1200.
20 (a) D. Visinescu, A. M. Madalan, M. Andruh, C. Duhayon, J.-P. Sutter, L. Ungur, W. Van de Heuvel, L. F. Chibotaru, *Chem. Eur. J.*, 2009, **15**, 11808; (b) D. Visinescu, I. R. Jeon, A. M. Madalan, M. G.

Alexandru, B. Jurca, C. Mathonière, R. Clérac, M. Andruh, *Dalton Trans.*, 2012, **41**, 13578.

21 (a) M. G. Alexandru, D. Visinescu, A. M. Madalan, F. Lloret, M. Julve, M. Andruh, *Inorg. Chem.*, 2012, **51**, 4906; (b) M.-G. Alexandru, D. Visinescu, M. Andruh, N. Marino, D. Armentano, J. Cano, F. Lloret, M. Julve, *Chem. Eur. J.*, 2015, **21**, 5429.

22 M. X. Yao, Q. Zheng, K. Qian, Y. Song, S. Gao, J. L. Zuo, *Chem. Eur. J.*, 2013, **19**, 294.

23 (a) W.-B. Sun, P.-F. Yan, G.-M. Li, J.-W. Zhang, T. Gao, M. Suda, Y. Einaga, *Inorg. Chem. Comm.*, 2010, **13**, 171; (b) T. Gao, P.-F. Yan, G.-M. Li, J.-W. Zhang, W.-B. Sun, M. Suda, Y. Einaga, *Solid State Sci.*, 2010, **12**, 597; (c) K.-Q. Hu, X. Jiang, S.-Q. Wu, C.-M. Liu, A.-L. Cui, H.-Z. Kou, *Inorg. Chem.*, 2015, **54**, 1206.

24 (a) M. Sakamoto, K. Manseki, H. Okawa, *Coordin. Chem. Rev.*, 2001, **219-221**, 379; (b) H. Okawa, H. Furutachi, D. E. Fenton, *Coordin. Chem. Rev.* 1998, **174**, 51; (c) P. A. Vigato, V. Peruzzo, S. Tamburini, *Coordin. Chem. Rev.,* 2012, **256**, 953; (d) P. A. Vigato, S. Tamburini, L. Bertolo, *Coordin. Chem. Rev.*, 2007, **251**, 1311.

25 M. Andruh, J.-P. Costes, C. Diaz, S. Gao, *Inorg. Chem.*, 2009, **48**, 3342.

26 (a) J. D. Rinehart, J. R. Long, *Chem. Sci*., 2011, **2**, 2078; (b) L. Sorace, C. Benelli, D. Gatteschi, *Chem. Soc. Rev.*, 2011, **40**, 3092; (c) J. Luzon, R. Sessoli, *Dalton Trans.*, 2012, **41**, 13556; (d) F. Habib, M. Murugesu, *Chem. Soc. Rev.*, 2013, **42**, 3278; (d) D. N. Woodruff, R. E. P. Winpenny, R. A. Layfield, *Chem. Rev.*, 2013, **113**, 5110; (e) H. L. C. Feltham, S. Brooker, *Coordin. Chem. Rev.*, 2014, **276**, 1.

27 (a) J.-P. Costes, F. Dahan, W. Wernsdorfer, *Inorg. Chem.*, 2006, **45**, 5; (b) T. Kajiwara, M. Nakano, S. Takaishi, M. Yamashita, *Inorg. Chem.*, 2008, **47**, 8604; (c) T. Yamaguchi, J.-P. Costes, Y. Kishima, M. Kojima, Y. Sunatsuki, N. Bréfuel, J.-P. Tuchagues, L. Vendier, W. Wernsdorfer, *Inorg. Chem.*, 2010, **49**, 9125; (d) T. D. Pasatoiu, J.-P. Sutter, A. M. Madalan, F. Z. C. Fellah, C. Duhayon, M. Andruh, *Inorg. Chem.*, 2011, **50**, 5890.

28 (a) X.-Y. Wang, C. Avendaño, K. R. Dunbar, *Chem. Soc. Rev.*, 2011, **40**, 3213; (b) B. Sieklucka, R. Podgajny, T. Korzeniak, B. Nowicka, D. Pinkowicz, M. Koziel, *Eur. J. Inorg. Chem.*, 2011, 305.

29 D. Visinescu, C. Desplanches, I. Imaz, V. Bahers, R. Pradhan, F. A. Villamena, P. Guionneau, J.-P. Sutter, *J. Am. Chem. Soc.*, 2006, **128**, 10202.

30 B. Nowicka, T. Korzeniak, O. Stefanczyk, D. Pinkowicz, S. Chorazy, R. Podgajny, B. Sieklucka, *Coord. Chem. Rev.*, 2012, **256**, 1946.

31 C. R. Dennis, A. J. van Wyck, S. S. Basson, J. G. Leipoldt, *Transition Met. Chem.* 1992, **17**, 471.

32 (a) T. Kajiwara, K. Takahashi, T. Hiraizumi, S. Takaishi, M. Yamashita, *Polyhedron*, 2009, **28***,* 1860; (b) B. Cristóvão, J. Kłak, B. Miroslaw, L. Maz, *Inorg. Chim. Acta*, 2011, **378**, 288; (c) T. Kajiwara, M. Nakano, K. Takahashi, S. Takaishi, M. Yamashita, *Chem. Eur. J.*, 2011, **17**, 196; (d) T. Shiga, H. Miyasaka, M. Yamashita, M. Morimoto, M. Irie, *Dalton Trans.*, 2011, **40**, 2275; (e) L. Fei, Z. Fang, *Acta Cryst.*, 2008, **E64**, m406; (f) T. Ishida, R. Watanabe, K. Fujiwara, A. Okazawa, N. Kojima, G. Tanaka, *Dalton Trans.*, 2012, **41**, 13609.

33 A. M. Madalan, N. Avarvari, M. Fourmigué, R. Clérac, L. F. Chibotaru, S. Clima, M. Andruh, *Inorg. Chem.*, 2008, **47**, 940.

34 W.-B. Sun, P.-F. Yan, G.-M. Li, G.-F. Hou, *Acta Cryst. E*, 2009, **65**, m780.

35 N. Senyüz, Ç. Yüksektepe, H. Batu, N. Çaliskan, O. Büyükgüngör, *J. Chem. Crystallogr.*, 2010, **40**, 989.

36 W.-B. Sun, P.-F. Yan, G.-M. Li, J.-W. Zhang, T. Gao, M. Suda, Y. Einaga, *Inorg. Chem. Commun.*, 2010, **13**, 171.

37 (a) S. Chorazy, K. Nakabayashi, S.-i. Ohkoshi, B. Sieklucka, *Chem. Mater.*, 2014, **26**, 4072; (b) E. Chelebaeva, J. Long, J. Larionova, R. A. S. Ferreira, L. D. Carlos, F. A. Almeida Paz, J. B. R. Gomes, A. Trifonov, C. Guérin, Y. Guari, *Inorg. Chem.*, 2012, **51**, 9005.

38 (a) J.-P. Sutter, M. L. Kahn, S. Golhen, L. Ouahab, O. Kahn, *Chem. Eur. J.*, 1998, **4**, 571; (b) M. Zhu, P. Hu, Y. Li, X. Wang, L. Li, D. Liao, V. M. L. Durga Prasad Goli, S. Ramasesha, J.-P. Sutter, *Chem. Eur. J.*, 2014, **20**, 13356.

39 (a) J. Long, L. M. Chamoreau, V. Marvaud, *Dalton Trans.*, 2010, **39**, 2188; (b) T. Shiga, H. Miyasaka, M. Yamashita, M. Morimoto, M. Irie, *Dalton Trans.*, 2011, **40**, 2275; (c) T. Ishida, R. Watanabe, K. Fujiwara, A. Okazawa, N. Kojima, G. Tanaka, S. Yoshii, H. Nojiri, *Dalton Trans.*, 2012, **41**, 13609; (c) T. Kajiwara, K. Takahashi, T. Hiraizumi, S. Takaishi, M. Yamashita, *Polyhedron*, 2009, **28**, 1860; (d) T. Kajiwara, M. Nakano, K. Takahashi, S. Takaishi, *Chem. Eur. J.*, 2011, **17**, 196; (e) J.-P. Costes, F. Dahan, W. Wernsdorfer, *Inorg. Chem.*, 2006, **45**, 5; (f) X. Feng, W. Zhou, Y. Li, H. Ke, J. Tang, R. Clérac, *Inorg. Chem.*, 2012, **51**, 2722; (g) T. Kajiwara, M. Nakano, S. Takaishi, M. Yamashita, *Inorg. Chem.*, 2008, **47***,* 18604; (h) B. Cristóvão, K. Kłak, B. Miroslaw, R. Mazur, *Inorg. Chim. Acta*, 2011, **378**, 288; (i) R. Koner, H.-H. Lin, H.-H. Wei, S. Mohanta, *Inorg. Chem.*, 2005, **44**, 3524.

40 (a) F. Luis, J. Bartolomé, J. F. J. Fernández, J. M. Tejada, Hernández, X. X. Zhang, R. Ziolo, *Phys. Rev. B*, 1997, **55**, 11448; (b) J. Bartolomé, G. Filoti, V. Kuncser, G. Schinteie, V. Mereacre, C. E. Anson, A. K. Powell, D. Prodius, C. Turta, *Phys. Rev. B*, 2009, **80**, 014 430.

41 (a) T. Korzeniak, C. Desplanches, R. Podgajny, C. Giménez-Saiz, K. Stadnicka, M. Rams, B. Sieklucka, *Inorg. Chem.*, 2009, **48**, 2865; (b) R. Podgajny, R. Pełka, C. Desplanches, L. Ducasse, W. Nitek, T. Korzeniak, O. Stefanczyk, M. Rams, B. Sieklucka, M. Verdaguer, *Inorg. Chem.*, 2011, **50**, 3213.

42 C.J. O'Connor, *Prog. Inorg. Chem.*, 1982, **29**, 203.

43 J.-P. Costes, F. Dahan, A. Dupuis, J.-P. Laurent, *Chem. Eur. J.*, 1998, **4**, 1616.

44 (a) M. L. Kahn, R. Ballou, P. Porcher, O. Kahn, J.-P. Sutter, *J. Am. Chem. Soc.*, 2000, **122**, 3413. (b) M. L. Kahn, R. Ballou, P. Porcher, O. Kahn, J.-P. Sutter, *Chem. Eur. J.*, 2002, **8**, 525. (c) V. Chandrasekhar, T. Senapati, A. Dey, S. Das, M. Kalisz, R. Clérac, *Inorg. Chem.*, 2012, **51**, 2031.

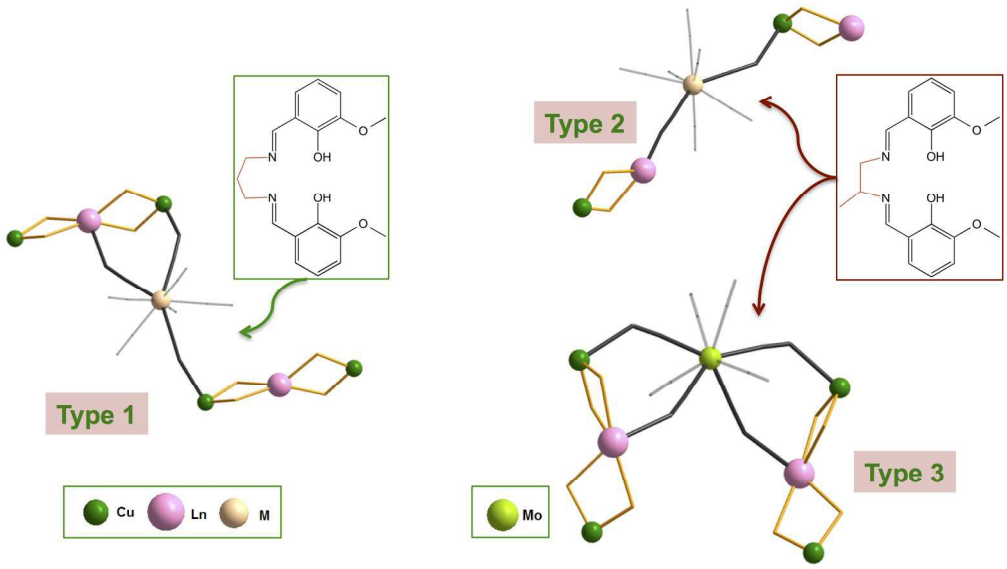

244x139mm (300 x 300 DPI)